

# An ATBD for the ENVISAT radiometer MERIS

---

Determination of aerosol optical thickness over land surfaces, using Bremen Aerosol Retrieval (BAER) and its applications to atmospheric correction over lands

For the attention of: Peter REGNER, ESA/ESRIN  
Luc GOVAERT, ESA/ESRIN

	Function	Name	Signature	Date
Prepared by	Project Engineer	W. Von Hoyningen-Huene, Béatrice Berthelot, A. Kokhanovsky and J.P. Burrows		
Verified by	Project Manager	Béatrice BERTHELOT		
Authorised by	General Manager	Richard BRU		





An ATBD for the ENVISAT radiometer MERIS

Ref	NOV-3341-NT-3352		
Issue	1	Date	03/11/05
Rev	0	Date	29/03/06
Page	3		

## Indexing form

<b>Customer</b>	<b>ESRIN</b>	<b>Contract N°</b>	<b>AO/1-4233/02/I-LG</b>	
<b>Confidentiality codes</b>			<b>Document management</b>	
Company / Programme		Defence		
Non-protected	<input type="checkbox"/>	Non-protected	<input checked="" type="checkbox"/>	None
Reserved	<input checked="" type="checkbox"/>	Limited diffusion	<input type="checkbox"/>	Internal
Confidential	<input type="checkbox"/>	Defence confidentiality	<input type="checkbox"/>	Customer
<b>Contractual document</b>		<b>Project N°</b>	<b>Work Package</b>	
Yes	<input checked="" type="checkbox"/>	3341	WP100	
No	<input type="checkbox"/>			
An ATBD for the ENVISAT radiometer MERIS				
Determination of aerosol optical thickness over land surfaces, using Bremen Aerosol Retrieval (BAER) and its applications to atmospheric correction over lands				
<b>Summary</b>				
This document describes the retrieval of aerosol optical thickness and surface reflectances from MERIS Level 2 data over land.				
<b>Document</b>				
File name	NOV-3341-NT-3352_v1.0.doc		Nbr of pages	62
Project	MERIS		Nbr of tables	6
Software	Microsoft Office Word		Nbr of figures	18
Language	English		Nbr of appendices	0
<b>Document reference</b>				
Internal	NOV-3341-NT-3352		Issue	1
External	-		Date	03/11/05
			Revision	0
			Date	29/03/06
<b>Author(s)</b>		<b>Verified by</b>	<b>Authorised by</b>	
W. Von Hoyningen-Huene, Béatrice Berthelot, A. Kokhanovsky and J.P. Burrows		Béatrice BERTHELOT	Richard BRU	



An ATBD for the ENVISAT radiometer MERIS

Ref	NOV-3341-NT-3352		
Issue	1	Date	03/11/05
Rev	0	Date	29/03/06
Page	4		

---

## *Distribution list*

<b>INTERNAL</b>	<b>EXTERNAL</b>	
<b>Name</b>	<b>Name</b>	<b>Company / Organisation</b>
Documentation NOVELTIS	P.REGNER	ESA/ESRIN
Richard BRU	L. GOVAERT	ESA/ESRIN
Béatrice BERTHELOT	W VON HOYNINGEN-HUENE	Bremen University
	A. KOKHANSKY	Bremen University
	J. P. BURROWS	Bremen University





Ref	NOV-3341-NT-3352		
Issue	1	Date	03/11/05
Rev	0	Date	29/03/06
Page	6		

## Table of contents

<b>1. INTRODUCTION.....</b>	<b>12</b>
1.1. PURPOSE.....	12
1.2. ALGORITHM IDENTIFICATION .....	12
1.3. SCOPE.....	12
1.4. REVISION HISTORY .....	13
1.5. OTHER RELEVANT DOCUMENTS.....	13
<b>2. ALGORITHM OVERVIEW .....</b>	<b>15</b>
2.1. INTRODUCTION.....	15
2.2. OBJECTIVES.....	15
2.2.1. <i>Aerosol characterisation</i> .....	15
2.2.2. <i>Surface reflectances</i> .....	16
2.3. STATE IN AEROSOL RETRIEVAL FROM SATELLITE MEASUREMENTS .....	17
2.4. STATE IN ATMOSPHERIC CORRECTIONS METHOD USED FROM SATELLITE MEASUREMENTS.....	18
2.5. INSTRUMENT AND DATA CHARACTERISTICS .....	18
2.6. RETRIEVAL STRATEGY .....	20
2.6.1. <i>Step 1: Cloud screening improvement</i> .....	20
2.6.2. <i>Step 2: BAER method</i> .....	20
2.6.3. <i>Step 3: Atmospheric correction method</i> .....	20
<b>3. ALGORITHM DESCRIPTION .....</b>	<b>21</b>
3.1. THEORETICAL DESCRIPTION .....	21
3.1.1. <i>BAER method for SeaWifs</i> .....	21
3.1.2. <i>Adaptation to MERIS</i> .....	23
3.1.3. <i>Integrated BAER program general flow chart</i> .....	24
3.2. MATHEMATICAL DESCRIPTION OF THE ALGORITHM .....	25
3.2.1. <i>Cloud Screening</i> .....	25
3.2.2. <i>Aerosol optical thickness estimation</i> .....	29
3.2.3. <i>Atmospheric Correction and Determination of Surface Reflectance</i> .....	44
<b>4. RESULTS AND CONCLUSION.....</b>	<b>48</b>
4.1. RESULTS OF THE APPROACH .....	48
4.2. VALIDATION PLAN .....	51
4.3. CONCLUSION, OUTLOOK .....	51
<b>5. ASSUMPTIONS AND LIMITATIONS.....</b>	<b>53</b>
5.1. ASSUMPTIONS .....	53
5.1.1. <i>Aerosol optical thickness estimation</i> .....	53
5.1.2. <i>Surface reflectance estimation</i> .....	53
5.2. LIMITATIONS.....	53
<b>6. PRACTICAL CONSIDERATIONS.....</b>	<b>54</b>
6.1. INTEGRATOR PROCESSOR USER’S GUIDE.....	54
6.1.1. <i>Software and hardware requirement</i> .....	54
6.1.2. <i>Integrated BAER processor Set Up</i> .....	54
6.1.3. <i>Overview of the user interface</i> .....	55
6.1.4. <i>Data management</i> .....	55
6.1.5. <i>Option activation</i> .....	55
6.2. INTEGRATED PROCESSOR INPUT/OUTPUT .....	56
6.2.1. <i>Input data</i> .....	56



An ATBD for the ENVISAT radiometer MERIS	Ref	NOV-3341-NT-3352		
	Issue	1	Date	03/11/05
	Rev	0	Date	29/03/06
	Page	7		

6.2.2. *Output data* ..... 56  
6.2.3. *Naming convention* ..... 57

**7. REFERENCES**..... **59**

Ref	NOV-3341-NT-3352		
Issue	1	Date	03/11/05
Rev	0	Date	29/03/06
Page	8		

## List of figures

FIGURE 1: EXAMPLE OF AOT RETRIEVAL FROM SEAWIFS, SHOWING FIRE PLUMES OF THE FOREST FIRES IN PORTUGAL FOR AUGUST 12, 2003. ....	22
FIGURE 2: SCHEME OF THE PLACE OF BAER WITHIN THE PROCESS OF ATMOSPHERIC CORRECTION OVER LAND SURFACES. ....	24
FIGURE 3: REPRESENTATION OF A SUB PIXEL CLOUD IN A PIXEL. ....	25
FIGURE 4: VARIATION OF THE TOA REFLECTANCE IN PRESENCE OF SUB PIXEL CLOUD. ....	26
FIGURE 5: VARIATION OF AOT RETRIEVAL WITH CLOUD FRACTION ....	26
FIGURE 6: SPECTRAL TOA REFLECTANCE FOR CLEAN CONTINENTAL AEROSOL MODEL (RED SOLID LINE) AND A THIN CI CLOUD (BLACK LINE) SEPARATELY AND THEIR COMPOSED EFFECT (BLUE LINE). FOR COMPARISON A MARINE AEROSOL MODEL FITS WITH THE COMPOSED CONDITIONS. ....	27
FIGURE 7: SCHEME OF THE RETRIEVAL PROCEDURE FOR THE AEROSOL OPTICAL THICKNESS OVER LAND: DETERMINATION OF THE AEROSOL REFLECTANCE SUBTRACTING THE SURFACE REFLECTANCE BY EQ. 3, DESCRIBED IN SECTIONS (3.2.2.1) AND (3.2.2.3), APPLICATION OF THE LUT AND THE CONSTRAINTS, DESCRIBED IN SECTIONS (3.2.2.5) AND (3.2.2.3). ....	30
FIGURE 8: SPECTRA USED FOR THE DETERMINATION OF THE APPARENT SPECTRAL SURFACE REFLECTANCE WITHIN THE BAER APPROACH: THE 'CASI2' SOIL SPECTRUM IS TAKEN FROM CASI-RADIOMETER MEASUREMENTS (OLBERT (1998)) AND THE KARNIELI2 DESERTIC SPECTRUM SOIL IS TAKEN FROM BARET (PERSONAL COMMUNICATION). THE VEGETATION SPECTRUM IS TAKEN FROM THE CAMELEO DATABASE, ESCADAFAL AND BOHBOT (1999). ....	35
FIGURE 9: SENSITIVITY OF AEROSOL REFLECTANCE TO DEVIATIONS OF THE SURFACE REFLECTANCE FROM THE CORRECT VALUE.....	38
FIGURE 10: AEROSOL PHASE FUNCTIONS OF THE CASES USED FOR THE LUT : (A) EXPERIMENTAL PHASE FUNCTIONS FROM LACE-98, CASES WITH INCREASED LATERAL SCATTERING (THICK BLACK CURVES, USED IN CASE 1 ), (B) 'AVERAGE CONTINENTAL' (CASE 3) AND 'CLEAN CONTINENTAL' (CASE 2) FROM OPAC. TWO MORE CASES ARE SHOWN IN THE PLOT 'DESERT' FROM OPAC AND 'CLEAN MARITIME' FROM OPAC.....	42
FIGURE 11: LUT FOR CASE 1: LACE-98 AEROSOL PHASE FUNCTION AND A SINGLE SCATTERING ALBEDO $\omega_0 = 0.98$ , FOR LAND SURFACE CONDITIONS FOR THE DIFFERENT CHANNELS OF MERIS.....	42
FIGURE 12: LUT FOR CASE 2, USING THE AEROSOL PHASE FUNCTION AND A SINGLE SCATTERING ALBEDO $\omega_0 = 0.975$ OF THE 'CLEAN CONTINENTAL' AEROSOL MODEL FROM OPAC 3.1 HESS <i>ET AL.</i> (1998), FOR LAND SURFACE CONDITIONS FOR THE DIFFERENT CHANNELS OF MERIS. ....	43
FIGURE 13 LUT FOR CASE 3 WITH AN AEROSOL PHASE FUNCTION AND A SINGLE SCATTERING ALBEDO $\omega_0 = 0.928$ OF THE 'AVERAGE CONTINENTAL' AEROSOL MODEL FROM OPAC 3.1 HESS <i>ET AL.</i> (1998), FOR LAND SURFACE CONDITIONS FOR THE DIFFERENT CHANNELS OF MERIS. ....	43
FIGURE 14: SCHEME OF THE RETRIEVAL PROCEDURE FOR THE SURFACE REFLECTANCES OVER LAND. ....	45
FIGURE 15: AEROSOL OPTICAL THICKNESS FOR CHANNEL 2 (0.443 $\mu\text{m}$ ) OVER SPAIN FROM MERIS L2 DATA, TAKEN AT 13. APRIL 2003, 10:10:45.....	49
FIGURE 16: COMPOSITION OF DIFFERENT SPECTRAL AOT, RETRIEVED FROM THE SCENE OVER FRANCE AND SPAIN FROM MERIS L2 DATA FOR THE 13. APRIL 2003. ....	50
FIGURE 17: SPECTRAL SURFACE REFLECTANCE OF DIFFERENT PLACES WITHIN THE SCENE OVER SPAIN FROM MERIS L2 DATA FOR THE 13. APRIL 2003.....	50
FIGURE 18: INTEGRATED BAER PROCESSOR PANELS .....	55





An ATBD for the ENVISAT radiometer MERIS	Ref	NOV-3341-NT-3352		
	Issue	1	Date	03/11/05
	Rev	0	Date	29/03/06
	Page	9		

---

*List of tables*

TABLE 1: MERIS SPECTRAL CHARACTERISTICS: BAND CENTRE AND WIDTH. .... 19

TABLE 2: TIE POINT INFORMATION CONTENT ..... 19

TABLE 3: SPECTRAL CHARACTERISTICS OF THE SELECTED COMPARABLE MERIS AND SEAWIFS CHANNELS FOR THE APPLICATION OF THE BAER APPROACH. CHANNELS IN BOLD ARE USED FOR THE BAER RETRIEVAL OF THE AOT AND THE DETERMINATION OF THE NDVI. .... 23

TABLE 4: POLYNOMIAL COEFFICIENTS FOR THE DETERMINATION OF THE TOTAL TRANSMISSIONS ..... 31

TABLE 5: POLYNOMIAL COEFFICIENTS FOR THE DETERMINATION OF THE HEMISPHERIC REFLECTANCE ..... 31

TABLE 6: GROUND-BASED AND RETRIEVED AOT OF THE SCENE OF THE 13. APRIL 2003 OVER SOUTHERN FRANCE AND SPAIN..... 49

## Acronyms

AAI	Aerosol Absorbed Index
AATSR	Advanced Along Track Scanning radiometer
ACE	Aerosol Characterisation experiment
AERONET	Aerosol Robotic Network
AOT	Aerosol Optical Thickness
ASCAR	Algorithm Survey and Critical Analysis Report
ATBD	Algorithm Theoretical Basis Document
ATSR-2	Along Track Scanning radiometer
AVHRR	Advances Very High Resolution Radiometer
BAER	Bremen AERosol algorithm for Meris
BEAM	Basic Envisat AATSR MERIS toolbox
DDV	Dark Dense Vegetation
DWD	Deutscher Wetterdienst
ENVISAT	ESA satellite
GOMETRAN	GOME radiative TRANSfer model
IGOS	Integrated Global Observing Strategy
IPCC	Intergovernmental Panel Climate Change
KNMI	Koninklijk Nederlands Meteorologisch Instituut
L1	Level 1
L2	Level 2
LACE	Lindenberg Aerosol Characterisation experiment
LUT	Look Up Table
MERIS	Moderate Imaging Spectrometer
MISR	MultiaNgle Imaging Spectrometer
MODIS	Moderate Resolution Imaging SpectroRadiometer
NIR	Near Infra Red
NDVI	Normalised Difference Vegetation Index
POLDER	Polarisation and Directionality of the Earth's Reflectances
RMSD	Root Mean Square Deviation
RTM	Radiative Transfer Model
SCIAMACHY	SCanning Imaging Absorption Spectrometer for Atmospheric CHartographY
SCIATRAN	SCIAMACHY radiative TRANSfer model
SeaWiFS	Sea Viewing Wide Field of View Sensor
SURF	Surface
SW	ShortWave
SW-VIS	Short Wave -Visible
TOMS	Total Ozone Mapping Spectrometer
VIS	Visible



Ref	NOV-3341-NT-3352		
Issue	1	Date	03/11/05
Rev	0	Date	29/03/06
Page	11		

---

## Abstract

This document describes the algorithm for remote sensing of aerosols from MERIS data over land. The algorithm has been developed to monitor the aerosol optical thickness (proportional to the aerosol total loading), over most of part of the continents. The aerosol information is used in a second step to perform atmospheric corrections of remotely sensed surface reflectance over the land.

The actual MERIS Level 2 product provides reflectance data with an incomplete atmospheric correction over land. The atmospheric correction is made for Rayleigh scattering and gases only and the variable aerosol influence is not considered. Thus an additional step of atmospheric correction for L2 data over land is required, considering the effect of the atmospheric aerosol. This includes (a) a cloud screening, (b) the retrieval of aerosol optical thickness (AOT) and (c) their application within an atmospheric correction procedure.

The original approach has been developed to retrieve the spectral aerosol optical thickness AOT over land from the looking multi-wavelength radiometer SeaWiFS L1 data, using top-of-atmosphere reflectance. For the retrieval of the MERIS AOT, the BAER (Bremen AErosol Retrieval) method is used and modified for the use with MERIS L2 data.

The method is based on the determination of the aerosol reflectance over 'dark surfaces', which is over land a vegetation covered land surfaces in the UV and short-wave-VIS range below the red-edge of the vegetation spectrum. This requires over land a proper separation of the variable surface effects, other atmospheric effects and aerosol effect. For L2 data over land, the variability of the vegetation cover and of the kind of the vegetation is considered dynamically by means of a surface reflectance model tuned from the satellite scene self by the NDVI. Removing the estimation of the surface effect the aerosol reflectance will be obtained. Look-up-tables of the relationship between AOT - aerosol reflectance and the use of constraints enable the determination of the AOT for 7 MERIS channels in a spectral range of 0.412 – 0.670  $\mu\text{m}$ .

For the atmospheric correction the AOT is extrapolated to the other channels by using Angström power law with parameters estimated from the retrieved AOT. Others terms of radiative transfer (aerosol reflectance, total transmittance and hemispheric reflectance) are computed once the AOT known to correct the Top Of Aerosol reflectance from aerosol effect.

The atmospheric correction step considers the effects of aerosol reflectance and total aerosol transmissions and gives the atmospherically corrected spectral surface reflectance either using the SMAC, Dedieu *et al*, 1994, or the integrated aerosol correction procedure UBAC (University Bremen Aerosol Correction), described within this ATBD.



Ref	NOV-3341-NT-3352		
Issue	1	Date	03/11/05
Rev	0	Date	29/03/06
Page	12		

# 1. Introduction

---

## 1.1. Purpose

The Algorithm Theoretical Basis Document (ATBD) describes an algorithm used to retrieve information both on the atmosphere (aerosol content and its characterisation) and properties of terrestrial surfaces (surfaces reflectances) from the analysis of Level 2 data generated by the Medium Resolution Imaging Radiometer (MERIS) of the European Space Agency (ESA) at both full and reduced resolution.

This document identifies the sources of input data, outlines the physical principles and mathematical background justifying the approach, describes the proposed algorithm, and lists the assumptions and limitations of the techniques.

## 1.2. Algorithm identification

The algorithm is called **Integrated BAER processor**. It chains three functions for the cloud screening, the aerosol estimation, and the atmospheric correction.

## 1.3. Scope

The Medium Resolution Imaging Spectrometer MERIS provides the top-of-atmosphere radiances in 15 channels in full resolution mode (300 m) and reduced resolution mode (1200m), of which 13 channels are used for land surface observations (Bezy *et al.*, 2000). At present time, ESA provides to the land user community a MERIS level 2 products which contains top of aerosol reflectances, i.e. reflectances corrected for Rayleigh scattering and gaseous absorption, but not for aerosol absorption and scattering. However, information about aerosol is provided in the products in the form of aerosol optical thickness and angstrom coefficient only over dark dense vegetation (DDV) surfaces (MERIS ATBD 2.15, Santer 2000).

The objective of this document is to provide a detailed description and justification of an algorithm proposed to retrieve aerosol information from MERIS observations (L2 data) over land, and its use into the atmospheric correction scheme.

The ESA requirement was to complete this at present incomplete atmospheric correction scheme over land surface and propose an algorithm for the aerosol correction, which can be integrated into the BEAM toolbox (BEAM, 2004). This shall enable the MERIS scientific user community

- a) to retrieve from MERIS Level 2 products estimates of the aerosol optical thickness and Angstrom coefficient over land surfaces;
- b) to actually perform the aerosol correction and derive atmospherically corrected surface reflectances in 13 spectral MERIS bands.

The document is structured as follows:

Section 1.3 explains the scope and objectives for aerosol retrievals from space-borne platforms and the current state in the method development. It provides an overview of the BAER (**B**remen **A**erosol **R**etrieval) approach and its application for atmospheric correction.

Section 2 gives the overview of the steps of the approach for the correction of aerosol effects.

Section 3 presents the three steps of the Integrated BAER algorithm: the cloud screening (section 3.2.1), the aerosol estimation (section 3.2.2) and the aerosol correction (section 3.2.3).

Section 4 summarizes some results of the prototype algorithm, (validation results are fully described in the separate validation report of BAER, c.f. BAER Validation report, 2006). It concludes on the key results and provides some recommendations for further algorithm improvements.

Section 5 provides with assumptions and limitations of the algorithm.

Section 6 describes the processor, and guides the user in the choice of options for the retrieval.

## 1.4. Revision history

The original document is referred by NOV-3160-NT-2703.doc dated January, 2005. This current version includes the latest developments and modifications made in the algorithm during its validation phase.

## 1.5. Other relevant documents

**Berthelot, B.**, Dedieu, G., 1997. Correction of atmospheric effects for VEGETATION data. Physical Measurements and Signatures in Remote Sensing, Guyot & Phulpin (eds), Balkema, Rotterdam, ISBN 90 5410 9173

Rahman H. and Dedieu G.: SMAC: a simplified method for the atmospheric correction of satellite measurements in the solar spectrum, International Journal of Remote Sensing, 1994, vol.15, No.1, 123-143.

**von Hoyningen-Huene, A.A.** Kokhanovsky, J.P. Burrows, **V. Bruniquel-Pinel, P. Regner, F. Baret**: Simultaneous Determination of Aerosol- and Surface Characteristics from Top-of-Atmosphere Reflectance using MERIS on board of ENVISAT. JASR 2006 (in press).

**von Hoyningen-Huene, W.**, Kokhanovsky, Burrows, J.P., **Berthelot, B., Regner, P., Baret, F.** (2005) Aerosol optical thickness retrieval over land: The atmospheric correction based on MERIS L2 reflectance. Proc. of MERIS/AATSR Workshop 2005, ESA ESRIN 26.-30. Sept. 2005, ESA SP-597, Dec. 2005.

**von Hoyningen-Huene, W** A.A. Kokhanovsky, J.P. Burrows, **V.Bruniquel, P. Regner**: State in aerosol remote sensing for atmospheric correction of MERIS land surface products. Proc. of ENVISAT/MERIS Workshop 2003, ESA ESRIN 10.-13.Nov. 2003, ESA SP-549, May 2004.

**von Hoyningen-Huene, W., Alexander A. Kokhanovsky, John P. Burrows, Prof. Dr.; Veronique Bruniquel-Pinel; Peter Regner, 2005a.** Simultaneous determination of aerosol- and surface characteristics from top-of-atmosphere reflectance using MERIS on board of ENVISAT J. *Adv. Space Res.* 32(2005) (accepted).



An ATBD for the ENVISAT radiometer MERIS	Ref	NOV-3341-NT-3352		
	Issue	1	Date	03/11/05
	Rev	0	Date	29/03/06
	Page	14		

- von Hoyningen-Huene, W., Kokhanovsky, A. A., Wuttke, M. W., Buchwitz, M., Gerilowski, N., Burrows, J. P., Latter, B., Siddans, B., Kerridge, B. J., 2005b.** Validation of SCIAMACHY top-of-atmosphere reflectance for aerosol remote sensing using MERIS L1 data. *ACP (Special Issue SCIAMACHY validation)*. Accepted 2004.
- von Hoyningen-Huene, W., 2005c:** Cloud influence on satellite measurements of aerosol properties. In ACCENT AT-2, Report of the 3. AT-2 Workshop, Oberpfaffenhofen, 6.-8 June 2005, p. 45-50. [http://troposat.iup.uni-heidelberg.de/AT2/workshop/AT2\\_wks\\_3\\_report.pdf](http://troposat.iup.uni-heidelberg.de/AT2/workshop/AT2_wks_3_report.pdf)

## 2. Algorithm overview

---

### 2.1. Introduction

MERIS instrument on board ENVISAT launched in 2002 provides earth observations at a global scale in the spectral range [0.4- 0.9]  $\mu\text{m}$  on a daily basis. These observations are important to improve the understanding of the vegetation / climate interactions. However these observations integrate the contributions from the atmosphere and surface and the difficulty is to separate the two contributions to analyse and relate both signals to the main atmosphere and surface biophysical products.

There are several objectives for satellite observations of properties of atmospheric aerosols, especially the aerosol optical thickness (AOT) and surface reflectances. These are:

Atmospheric correction for surface remote sensing (both over ocean and land):

- ◆ The knowledge and regional variability of the AOT enables the determination of the spectral surface reflectance, required for land use applications.

Climate research:

- ◆ The determination of the direct radiative effect of the aerosol is based directly on the knowledge of the AOT. Moreover this, the aerosol has indirect effects on cloud formation by aerosol-cloud-interaction.

Environmental control:

- ◆ AOT is a good quantitative indicator for atmospheric pollution by particulate matter and the transport of these pollutants.

### 2.2. Objectives

#### 2.2.1. Aerosol characterisation

A quantitative key parameter as basis for many other applications is the aerosol optical thickness. Aerosol is an important atmospheric constituent, affecting several aspects of climate, atmospheric chemistry, environmental pollution, health aspects for the population and others. IPCC (2002) and IGOS (2004) reports document the importance of the knowledge of aerosol parameters for different purposes, as air quality monitoring, climate forcing and analysis of tropospheric and stratospheric chemistry. The reports highlight the urgent need for a quantitative determination of the aerosol optical thickness (AOT), aerosol absorption, and other derived aerosol parameters. Specifically climate research, environmental control and atmospheric correction of land and ocean surface data require the knowledge of:

- ◆ Spatial and regional variability of the aerosol over land and ocean
- ◆ Temporal variability
- ◆ Sources and sinks of aerosols
- ◆ Types of aerosols

Aerosol exhibits high spatial and temporal variability in the atmosphere. This is caused by the different sources, the variability of its physico-chemical composition and its interaction with the humidity. Therefore aerosol investigation for climate research and environmental control requires the identification of source regions, their strength and aerosol type, the determination of the variable turbidity state of regions and information on the transformation of aerosol types at long range transports of aerosols on regional and global scales. This can be retrieved from with space-borne measurements, if adequate methods are available, yielding also global data.

Consequently, there is an urgent need for methods of space-borne aerosol determination, enabling the retrieval of AOT and their spectral properties, IGOS (2004). Space-borne observations enable a regional and global view with an appropriate temporal repetition frequency and provide key information to scientists and decision and policy makers on aerosol properties, their variability and trends in their distribution.

Satellite observations with nadir scanning radiometers can provide the regional and temporal distribution of AOT and their spectral behaviour gives some indications for the prevailing aerosol type. Since the most aerosol sources are over land, retrieval methods are required to give the AOT not only over ocean surfaces with low and less variable surface reflectance, but also over land.

Retrieval methods must be able to detect the AOT also over more variables land surfaces. This enables observations of aerosol effects of anthropogenic pollution, mineral dust, biomass burning and the state of general atmospheric turbidity caused by aerosols. The latter enables an atmospheric correction considering the variability of the aerosol effect, which is required for investigations of land use and its variation free of atmospheric effects. The determination of the AOT over land requires low and known surface reflectance. Over land, lower values for the surface reflectance are given in the green and blue bands of the spectrum. Therefore, the determination of AOT will be made mostly for wavelengths below 0.670  $\mu\text{m}$ .

Multi-spectral satellite instruments, like SeaWiFS, MERIS and MODIS provide sufficient spectral information to separate surface and aerosol contribution from the top-of-atmosphere reflectance. This separation needs a-priori knowledge about the surface reflectance, estimable from multi-spectral satellite observations.

The determination of the wavelength-dependence of this parameter with sufficient accuracy and within an appropriate spectral range enables the determination of a series of other aerosol characteristics, such as the Angström parameter, the aerosol type, the effective radius and the aerosol concentration. MERIS has sufficient spectral channels within the visible spectral range that can be used for the determination of the spectral behaviour of the AOT. The key problem here is the fact, that the AOT is influenced by the spectral surface reflectance characteristics of the underlying surface.

### 2.2.2. Surface reflectances

The generation of biophysical products such as LAI, fAPAR, and fCover, vegetation indices from remote sensing data requires the use of Top Of Canopy reflectances (or surface reflectances) as input of algorithms. The accuracy of the surface reflectances depends mainly on the accuracy of the atmospheric correction scheme (Out of calibration), so that the accuracy of vegetation products is strongly linked to that of previous step of the data processing.





Ref	NOV-3341-NT-3352		
Issue	1	Date	03/11/05
Rev	0	Date	29/03/06
Page	17		

MERIS L2 reflectance data over land are a non uniform product. Over water, they give the water leaving reflectance, because atmospheric correction is made completely for all atmospheric constituents, including aerosols. Over land only Rayleigh scattering and gaseous absorption is considered, and the aerosol effect remained unconsidered. Therefore the focus of this document was on the aerosol correction of MERIS L2 data. However, the approach can be applied generally for the consideration of aerosol effects.

### 2.3. State in Aerosol Retrieval from Satellite Measurements

The present techniques for the retrieval of aerosol parameters from space borne measurements are mostly restricted to dark ocean surfaces using NIR channels (AVHRR, SeaWiFS, MODIS, MERIS). The relatively low spectral surface reflectance of the ocean can be neglected [cf. Husar *et al.*, 1997; Moulin *et al.*, 1997; Nakajima and Higurashi, 1997; Tanré *et al.*, 1999; Deuzé *et al.*, 1999; Goloub *et al.*, 1999; Geogdzhayev *et al.*, 2002]. Over land, the absorbing aerosol index (AAI) and estimates of the optical depth in the UV from TOMS yield information about the existence of strongly absorbing aerosols overland and ocean [cf. J. R. Herman *et al.*, 1997a, 1997b; Torres *et al.*, 1998]. The transfer of the AAI to quantitative aerosol parameters as an aerosol optical thickness requires several model assumptions [cf. Torres *et al.*, 1998, 2002]. This index, generally do not provide a quantitative aerosol information in terms of an aerosol optical thickness (AOT). At best, they provide limited information for very strong special aerosol events, as discussed in Bhartia *et al.* (1998), Torres *et al.* (2002).

The dual-view-technique from ATSR-2 (Veefkind *et al.*, 1999), AATSR and the multi-viewing technique of MISR or the angular scan of polarization information by POLDER, (Herman *et al.*, 1997b) allowed to retrieve also AOT over land surfaces. This technique has been shown as a powerful tool in aerosol remote sensing and has been extended to MISR to up to nine viewing geometries for the same ground target.

Concerning modern multichannel space-borne radiometers such as SeaWiFS, MODIS, SCIAMACHY, Kaufman *et al.* [1997a, 1997b; 2000] summarized the state and problems in aerosol retrieval and finally concluded that polar orbiting satellites will be able to estimate the daily aerosol properties.

The 'inter-correlation' - approach, Kaufman *et al.*, (1997), especially for MODIS uses empirical correlations between the channel at 2.1  $\mu\text{m}$  and 0.46  $\mu\text{m}$  or the other SW channels of MODIS. Thus, the variability of the surface reflectance in the blue channel of MODIS can be determined over a wide variety of land surfaces and the retrieval of the AOT performed. These empirical relationships were derived from AVIRIS. However, this information of the 2.1  $\mu\text{m}$  channels does not exist for MERIS and other ocean colour radiometers and another way for the estimation of the surface reflectance has to be gone. Santer *et al.* -approach 1999, 2000) restrict the retrieval of AOT to DDV ('dark dense vegetation') pixels with the result that the AOT can be obtained only at few dark targets, and large areas without aerosol information remain in the final product. The method has been developed for the exploitation of MERIS data in the ENVISAT ground segment.

A tuned mixing of land surface reflectance spectrum, using the NDVI and two basic surface types 'bare soil' and 'green vegetation' is used by the BAER approach (Bremen AEROSOL Retrieval, von Hoyningen-Huene *et al.*, 2003), to estimate the SeaWiFS spectral surface reflectance for wavelengths < 0.67  $\mu\text{m}$ . This approach is working also over a wide variety of land surfaces with different degrees of vegetation cover, given by the NDVI (Normalized Differential Pigment Index).



An ATBD for the ENVISAT radiometer MERIS	Ref	NOV-3341-NT-3352		
	Issue	1	Date	03/11/05
	Rev	0	Date	29/03/06
	Page	18		

These available approaches for aerosol correction are fully described in an ASCAR (Algorithm Survey and Critical Analysis Review) document, (ASCAR, 2003).

## 2.4. State in atmospheric corrections method used from Satellite Measurements

Atmospheric correction of satellite measurements is a major step in the retrieval of surface reflective properties. It involves removing the effect of gaseous absorption as well as correcting for the effect of an atmospheric molecular and particulate scattering.

Radiative transfer model allow to correct with accuracy the molecular scattering, and the aerosol scattering, if the aerosol properties are well known (at least aerosol type, and the quantity of aerosol in the atmosphere through the aerosol optical thickness).

For instance, the Moderate-Resolution Atmospheric Radiance and Transmittance Model-4 (MODTRAN-4) radiative transfer model (Berk *et al.* 2001), the 6S radiative transfer code (Vermote *et al.*, 1997) can be used to correct the TOA reflectance/radiances from the aerosol however, the correction is time consuming and new methods based on empirical, semi empirical modelling, Look Up Tables are proposed to allow the processing of huge amount of data. The objectives of our study are to develop fast, but accurate semi-analytical atmospheric correction scheme suitable for implementation in operational data processing of satellite narrowband observations

## 2.5. Instrument and data characteristics

The Medium Resolution Imaging Spectrometer (MERIS) is a programmable, medium-spectral resolution, imaging spectrometer operating in the reflected solar radiation spectral range. Fifteen spectral bands are routinely acquired in the 390 nm to 1040 nm spectral range (see Table 1).

The instrument scans the Earth's surface by the so called "push-broom" method. Linear CCD arrays provide spatial sampling in the across-track direction, while the satellite's motion provides scanning in the along-track direction. MERIS is designed so that it can acquire data over the Earth whenever illumination conditions are suitable. The instrument's 68.5° field of view around nadir covers a swath width of 1150 km.

The instrument acquires data in Reduced Resolution mode (RR) and Full Resolution mode (FR). The spatial resolution is about 1200 m in RR mode and 300 m in FR mode. An example of MERIS data in both resolutions over the same area is shown in over the Southeast of Spain, in 2003 (July 14).

While the observed radiances are available with the cited spatial resolution, auxiliary data are delivered at so-called tie points (Table 2) that are available with a resolution of roughly 16 km in both modes

**Table 1: MERIS spectral characteristics: band centre and width.**

#	Centre (nm)	Width (nm)	Potential Applications
1	412.5	10	Yellow substance and detrital pigments
2	442.5	10	Chlorophyll absorption maximum
3	490	10	Chlorophyll and other pigments
4	510	10	Suspended sediment, red tides
5	560	10	Chlorophyll absorption minimum
6	620	10	Suspended sediment
7	665	10	Chlorophyll absorption and fluo. reference
8	681.25	7.5	Chlorophyll fluorescence peak
9	708.75	10	Fluo. Reference, atmospheric corrections
10	753.75	7.5	Vegetation, cloud
11	760.625	3.75	Oxygen absorption R-branch
12	778.75	15	Atmosphere corrections
13	865	20	Vegetation, water vapour reference
14	885	10	Atmosphere corrections
15	900	10	Water vapour, land

**Table 2: Tie point information content**

parameter	Unit and origin
Latitude of the tie points	(1e-6) degrees
Longitude of the tie points	(1e-6) degrees
DEM altitude of the tie points	m
DRM roughness	m
DEM latitude correction	(1e-6) degrees
Sun zenith angle	(1e-6) degrees
Sun azimuth angle	(1e-6) degrees
Viewing zenith angle	(1e-6) degrees
Viewing azimuth angle	(1e-6) degrees
Zonal wind	m*s-1
Meridional wind	m*s-1
Mean sea level pressure	hPa
Ozone	DU
Relative humidity	%

## 2.6. Retrieval strategy

The strategy for remote sensing of aerosol over the land from MERIS L2 is based on the method called BAER, which has first been developed by von Hoyningen Huene *et al.* (2003) for the SW-VIS channels of the SeaWiFS instrument taking into consideration variable surface reflectance conditions. This technique is applied in the frame of the MERIS L2 data processing for the determination of aerosol optical thickness over land and the completion of the atmospheric correction in MERIS land products.

The full processing procedure is subdivided into 3 steps:

1. Cloud screening
2. Retrieval of aerosol optical thickness by the BAER approach
3. Atmospheric correction of aerosol effects in L2 reflectance data over land, using SMAC (Simplified Model of Atmospheric Correction, c.f. Dedieu *et al.*, 1994) or UBAC (University Bremen Atmospheric Correction, this document)

### 2.6.1. Step 1: Cloud screening improvement

Because the determination of the AOT is very sensitive to cloud condition, a cloud screening method is implemented into the processor in order to remove the clouds that have not been detected by the L2 operational processor. The method is based on multiple threshold methods and is described in section 3.2.1.

### 2.6.2. Step 2: BAER method

The objective of our study is to develop a fast, but accurate semi-analytical atmospheric correction scheme suitable for implementation in the BEAM toolbox. The retrieval technique uses a separation technique between aerosol and land surface properties in the short-wave visible channels of the MERIS radiometer for wavelengths lower than 0.67  $\mu\text{m}$ . This technique is a special variant of the 'dark target' method (Kaufman *et al.*, 1997a, 1997b) with a dynamical estimation of the surface reflectance. The land surface reflectance here is estimated by a linear mixing model of vegetation and non-vegetation spectra, tuned by the normalized differential vegetation index (NDVI). By the elimination of surface reflectance, an aerosol reflectance can be defined, for which lookup tables (LUT) for the retrieval of the aerosol optical thickness are generated using radiative transfer model (RTM) calculations.

### 2.6.3. Step 3: Atmospheric correction method

Two atmospheric methods are proposed as options to the user to correct the MERIS L2 data from the aerosol scattering. The first option is the integrated part of the BAER method, which estimates in the same processing aerosol and surface reflectances. The second option is to perform the SMAC method (Berthelot and Dedieu, 1997) using the aerosol optical thickness estimated in step 2.

## 3. Algorithm description

### 3.1. Theoretical description

#### 3.1.1. BAER method for SeaWifs

The Bremen AERosol Retrieval approach (BAER) is a retrieval procedure for the determination of the aerosol optical thickness from top-of-atmosphere (TOA) reflectance with underlying land surface. It has been first developed for SeaWiFS L1 data, using the blue and short-wave channels below the ‘red edge’ of the green vegetation.

BAER developed for SeaWiFS data used the top of atmosphere reflectance in the eight spectral bands of the instrument (von Hoyningen-Huene *et al.* (2003)). The method was applied to SeaWiFS and MODIS measurements in Asia during the ACE-Asia experiment by Lee *et al.* (2004) and Lee *et al.* (2005), investigating aerosol transports. Kokhanovsky *et al.* (2004b) and von Hoyningen-Huene *et al.* (2004) used SeaWiFS data to study aerosol properties in different situations, like dust storms, forest fire plumes and the formation of clouds.

The basic equation, used in BAER is Eq. 1. This equation gives the aerosol reflectance  $\rho_{Aer}(\lambda)$ , derived from the TOA reflectance  $\rho_{TOA}(\lambda)$  measured by the satellite. For the determination of the aerosol reflectances, two influences have to be removed from the TOA reflectance: (a) effect of Rayleigh scattering – second line, (b) effect of earth surface – third line of Eq. 1.

$$\rho_{Aer}(\lambda) = \rho_{TOA}(\lambda) - T_{Ray}(\lambda, M(zs)) \cdot T_{Aer}(\lambda, M(zs)) \cdot \rho_{Ray}(\lambda, M(zo), M(zs), p_{surf}(z)) - \frac{T_{Ray}(\lambda, M(zo)) \cdot T_{Aer}(\lambda, M(zo)) T_{Ray}(\lambda, M(zs)) \cdot T_{Aer}(\lambda, M(zs)) A_{surf}(\lambda, zo, zs)}{1 - A_{surf}(\lambda, zo, zs) \rho_{Hem}(\lambda, zo)} \quad \text{Eq. 1}$$

- $T_{Ray}$ ,  $T_{Aer}$  are the total transmissions of the atmosphere,  $A_{Surf}$  the surface albedo and  $\rho_{Hem}$  the hemispheric reflectance of the system earth – atmosphere. Their determination is described in section 3.2.2.2.1 of this document.
- The Rayleigh scattering depends on the air pressure, which is associated with the surface elevation. Therefore, the pressure is calculated using a digital elevation model, associated with the satellite scene. For this purpose, the GTOPO30 data base is used.
- The spectral surface albedo, e.g. the surface reflectance is obtained by the spectral surface reflectance model.

For land surfaces, this model is described in section 3.2.2.3.1. It is a dynamical surface reflectance model, composing the actual apparent surface reflectance spectrum for the SW channels from a linear mixing of spectra of ‘green vegetation’ and ‘bare soil’, tuned by the NDVI (normalized differential vegetation index) and a scaling factor adapted to the reflectance conditions of the scene.

For ocean a similar model is used, however, the spectra of ‘clean ocean’ and ‘coastal’ water are mixed, using the NDPI (normalized differential pigment index).

One example of the BAER algorithm is demonstrated in Figure 1 for a SeaWiFS scene covering Spain and Portugal on the 12<sup>th</sup> of August 2003 showing forest fire plumes moving out from the land to the Atlantic and causing some aerosol-cloud interaction in their trajectory. In this case, the use of BAER with SeaWiFS L1 data enabled the investigation of the aerosol transport over both land and ocean.

Thus, applications and validations of BAER with different instruments are made to retrieve the regional pattern of the AOT in different situations over both ocean and land, c.f. von Hoyningen-Huene *et al.*, 2004, von Hoyningen-Huene *et al.*, 2005, Kokhanovsky *et al.*, 2004, Lee *et al.*, 2004, Lee *et al.*, 2005.

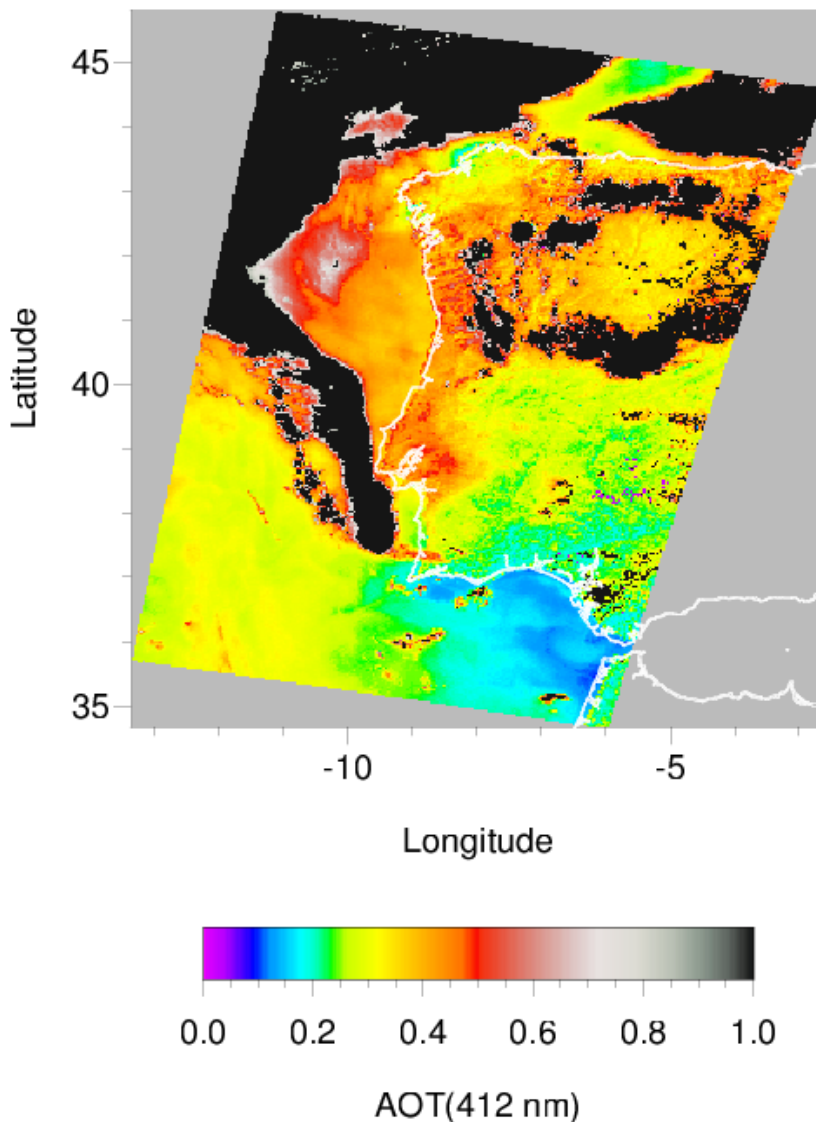


**Figure 1: Example of AOT retrieval from SeaWiFS, showing fire plumes of the forest fires in Portugal for August 12, 2003.**

### 3.1.2. Adaptation to MERIS

Since MERIS provides data of similar spectral and spatial resolution than SeaWiFS, a transfer of the BAER method to MERIS data is evident. However, the MERIS instrument has more channels covering a slightly broader spectral range than SeaWiFS (as shown in Table 3). Moreover, the greater number of spectral bands (13 versus 8), the differences in the width and in the center-wavelength have required the SeaWiFS BAER method a few adaptations to make it usable for MERIS data.

**Table 3: Spectral characteristics of the selected comparable MERIS and SeaWiFS channels for the application of the BAER approach. Channels in bold are used for the BAER retrieval of the AOT and the determination of the NDVI.**

MERIS				SeaWiFS		
Channel	Wavelength $\mu\text{m}$	Bandwidth Nm	Parameter	Channel	Wavelength $\mu\text{m}$	Bandwidth nm
1	0.4125	<b>10</b>	AOT	1	0.412	20
2	0.4425	<b>10</b>	AOT	2	0.440	20
3	0.490	<b>10</b>	AOT	3	0.490	20
4	0.510	<b>10</b>	AOT	4	0.510	20
5	0.560	<b>10</b>	AOT	5	0.555	20
6	0.620	10	AOT			
7	0.665	<b>10</b>	AOT, NDVI	6	0.670	20
8	0.6813	7.5				
9	0.705	10				
10	0.7538	7.5				
11	0.7606	3.8		7	0.765	40
12	0.775	15				
13	0.865	<b>20</b>	NDVI	8	0.865	40
14	0.885	10				
15	0.900	10				

The transfer to the method from Level 1 to MERIS level 2 data is described in the next section. Some improvements of BAER have been made compared with the first publication in 2003. Especially for heavy aerosol loadings, total transmissions and hemispheric reflectance are now implemented, improving the consideration of the surface contribution. Thus, BAER can also provide the required AOT input for an atmospheric correction of measured reflectance data to surface conditions.

The BAER algorithm has been adapted to the 13 MERIS channels, which are described in terms of wavelengths and bandwidths in Table 3. Channels 1 to 7 are used for the determination of the spectral AOT by BAER. This covers the spectral range of 0.412 to 0.665  $\mu\text{m}$ . Compared to the initial SeaWiFS BAER algorithm, there is one MERIS channel more that is useful for providing more spectral information of the AOT. This range is also used as basis for the extrapolation of the AOT to all 13 MERIS channels via the Angström coefficient needed for subsequent atmospheric correction.

The channels 11 and 15 are not used for the atmospheric correction, because they are strongly affected by gaseous absorption of  $\text{O}_2$  and  $\text{H}_2\text{O}$  vapour.

### 3.1.3. Integrated BAER program general flow chart

The Integrated BAER processing chain is shown in Figure 2. It contains three modules (grey part of the figure). Data processed are the standard MERIS L2 data, full or reduced resolution. The first module is a cloud detection module, which flags the clouds, in complement to the cloud flags provided with the L2 MERIS data. The second one is the BAER module which retrieves the AOT for seven short-wave channels of MERIS. From this information, the Angström parameter is then estimated and used to extrapolate the AOT for all 13 MERIS channels and to derive the aerosol reflectance needed to perform the atmospheric correction. The final output is the atmospheric corrected surface reflectance for 13 MERIS channels.

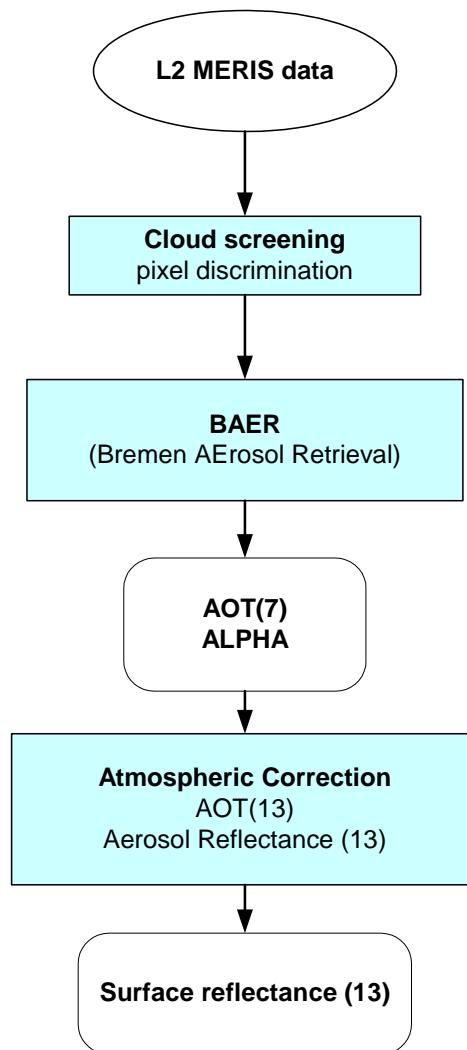


Figure 2: Scheme of the place of BAER within the process of atmospheric correction over land surfaces.



An ATBD for the ENVISAT radiometer MERIS	Ref	NOV-3341-NT-3352		
	Issue	1	Date	03/11/05
	Rev	0	Date	29/03/06
	Page	25		

## 3.2. Mathematical description of the algorithm

### 3.2.1. Cloud Screening

#### 3.2.1.1. Objectives

The determination of AOT and surface reflectances is very sensitive to cloud conditions. Clouds modify the scattered radiation, have an increased spectrally nearly neutral reflectance, so that they perturb the signal. In the case of thin clouds ( $C_i$ ) and fractional cloud coverage of few percent they are not recognized and could be considered as aerosols if they enter in the processing. Further clouds are elevated from surface.

Cloud identification is described in the ATBD 2.17, Santer *et al.*, 2000. Over land, identification and classification of homogeneous clouds is based on the apparent pressure in the  $O_2$  channel and thresholds on reflectance. This has been implemented into the ground segment for land, and clouds are flagged in the MERIS L2 Flag channel. However, until now, the quality of the product is not good enough and the pressure information not reliable enough. This is the reason why some new tests have been added to identify clouds into the Integrated BAER method.

#### 3.2.1.2. Sensitivity of the signal to cloud

##### 3.2.1.2.1 Impact of cloud fraction on the TOA signal

The disturbance involved by small clouds is illustrated hereafter. Fractional cloud cover in the satellite scene passes most cloud screening procedures (low cloud fractions: 1 ... 10%). It also depends on FOV, e.g. geometric resolution of the satellite instrument (Figure 3).

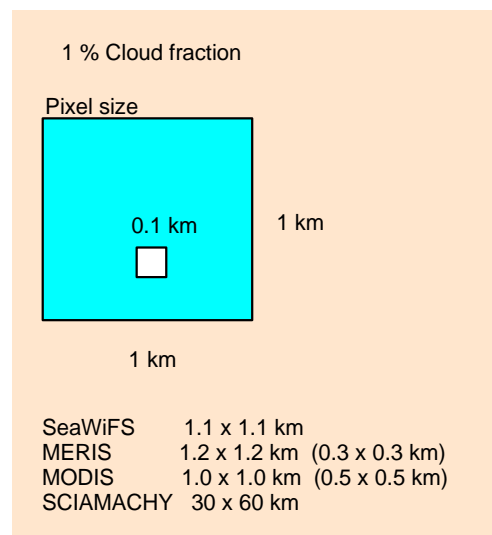


**Figure 3: Representation of a sub pixel cloud in a pixel.**

The sensitivity study to the sub pixel clouds has been made in order to quantify the errors introduced in the interpretation of the results when such a clouds is present in the medium resolution pixel, that is the case of MERIS, MODIS, SeaWiFS) and low resolution pixel (SCIAMACHY).

The influence of a sub pixel cloud is shown on Figure 4. The spectral variations of a top of atmosphere reflectance (TOA) are represented for different percent of cloud fraction (1 to 15%). The conditions of the simulations are indicated on the figure. Two effects are shown on this figure.

First, we see that the signal involves by only 1% cloud fraction of a Cu cloud changes continental aerosol of same AOT to marine model. Since thin Ci clouds have comparable reflectance range, like aerosols, the retrieval of aerosol Optical Thickness and aerosol type in this case will be biased.

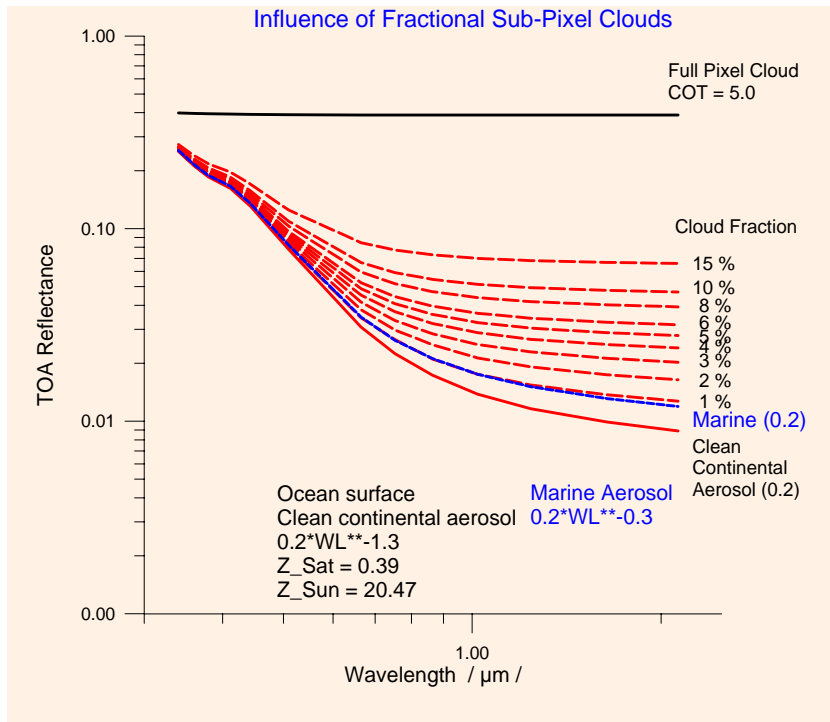


**Figure 4: Variation of the TOA reflectance in presence of sub pixel cloud.**

### 3.2.1.2.2 Impact on the AOT retrieval

The impact of cloud fraction on the AOT retrieval is shown on the next figure for three levels of continental aerosol optical thicknesses. The retrieval is clearly dependant of the cloud fraction. We see that 1% cloud fraction increases AOT with about 0.05.

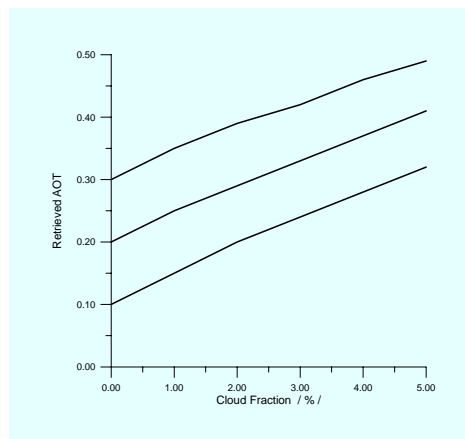


**Figure 5: Variation of AOT retrieval with cloud fraction**

The spectral variations of AOT are also modified when a high cirrus is present in the atmosphere. The Cirrus contamination yields also to aerosol of flatter spectral slope (Figure 6)

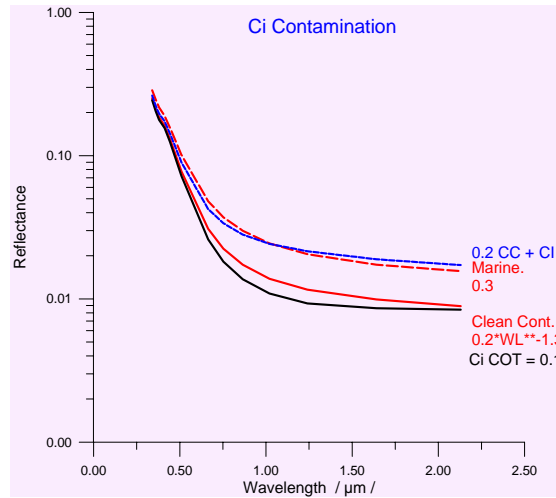


**Figure 6: Spectral TOA reflectance for clean continental aerosol model (red solid line) and a thin Ci cloud (black line) separately and their composed effect (blue line). For comparison a marine aerosol model fits with the composed conditions.**

### 3.2.1.3. Algorithm

In addition to the cloud identification provided with L2 MERIS data, new tests are added to detect the clouds.

#### Test 1: spectral dependence

Since clouds have a nearly spectrally neutral reflectance and the Rayleigh path reflectance is removed within the L2 Norm. rho\_surf - MDS (\*) data sets, fixed thresholds of a minimal cloud reflectance  $\rho_{cl}$  for the channels 2, 3 and 4 are used:

- $\rho_{cl}(2) = 0.2$ ,
- $\rho_{cl}(3) = 0.2$ ,
- $\rho_{cl}(4) = 0.2$ .

The value 0.2 is chosen from the minimum cloud reflectance, given by Kokhanovsky, 2004c.

#### Test 2: NDVI test

The second test is based on the NDVI value. If the NDVI is lower than a threshold (here 0.1), and the L2 reflectance in three channels greater than a threshold, then the pixel could be classified as cloudy. The tests are:

$$\text{if } \rho_{L2}(2) > 0.2 \quad \text{test}=\text{test}+1$$

$$\text{if } \rho_{L2}(3) > 0.2 \quad \text{test}=\text{test}+1$$

$$\text{if } \rho_{L2}(4) > 0.2 \quad \text{test}=\text{test}+1$$



An ATBD for the ENVISAT radiometer MERIS	Ref	NOV-3341-NT-3352		
	Issue	1	Date	03/11/05
	Rev	0	Date	29/03/06
	Page	28		

if NDVI > 0.1 (

if  $\rho_{L2}(13) > 0.53$       test=test+1

if  $\rho_{L2}(7) > 0.32$       test=test+1

if  $\rho_{L2}(3) > 0.30$       test=test+1      )

if test >=3      pixel = cloudy <b>Eq. 2</b>
--

MERIS pixels will be classified as cloudy, if three conditions are fulfilled among these six tests, the pixel is considered as cloudy.

The other pixels will be considered as cloud free and will be used for the aerosol retrieval.

### 3.2.1.4. Limitations

#### 3.2.1.4.1 High aerosol content

For a lot of cases this threshold is applicable. In cases of heavy aerosol loadings (forest fires, dust storms or heavy air pollution) this threshold is too restrictive and heavy aerosol events will be misclassified. For these particular cases, it is recommended to increase the threshold to 0.3 or even 0.4.

#### 3.2.1.4.2 Cirrus

Cases of thin cirrus clouds and small sub-pixel broken clouds of only few percent cloud fraction mostly will not really be recognized by the most cloud screening procedures. Their interference within the aerosol retrieval is discussed in von Hoyningen-Huene, 2005c.

#### 3.2.1.4.3 Cloud shadow impact

Especially, for lower sun elevations cloud shadow effects occur in the vicinity of clouds. Cloud shadows cover a fraction of atmosphere and surface. Thus, almost no scattering comes out of these shadowed parts of atmosphere. The scattered contribution of atmosphere consists of this fraction which comes from that part of atmosphere above the shadow region. Thus, Rayleigh path reflectance and aerosol reflectance is reduced compared with unshadowed regions. In such cases from L1 data TOA reflectances are obtained, which are smaller than Rayleigh path reflectance of the atmosphere. This criterion cannot be applied for L2 data, because Rayleigh scattering is there corrected and cannot be used as criterion. Here, 'unrealistic' low reflectance values should be excluded from processing. We tried different reflectance borders for this 'screening' with different effects. Values of these borders, which effectively remove cloud shadows, remove also some pixels which obviously are not affected by clouds. Thus, the cloud shadow screening is not an integrated component of BAER.

### 3.2.2. Aerosol optical thickness estimation

#### 3.2.2.1. Radiative Transfer and Aerosol

The retrieval of aerosol optical thickness is based on look-up-tables (LUT) describing the relationship between the aerosol reflectance  $\rho_{Aer}(\lambda)$ , determined by BAER, and the aerosol optical thickness  $\delta_A(\lambda)$ . This requires an adequate set of LUTs taking into account all factors which influence the radiative transfer in the atmosphere: i.e. illumination (solar zenith distance and azimuth) and observation geometry, Rayleigh scattering, surface reflectance for the different vegetation cover, the surface elevation with its surface pressure conditions, and finally the aerosol parameters including: aerosol phase function, aerosol optical thickness, aerosol single scattering albedo. The LUTs correspond to different aerosol types and are described in the section 3.2.2.5. The main task for an application of LUT is the separation of the aerosol reflectance out of the measured TOA.

The general equation of the determination of the aerosol reflectance is mainly based on the solution of the radiative transfer equation, given by Kaufman *et al.* (1997a), which is also applicable to MERIS L1b data.

$$\begin{aligned} \rho_{Aer}(\lambda) = & \rho_{TOA}(\lambda) \\ & - T_{Ray}(\lambda, M(z_S)) \cdot T_{Aer}(\lambda, M(z_S)) \cdot \rho_{Ray}(\lambda, M(z_O), M(z_S), p_{surf}(z)) \\ & \frac{T_{Ray}(\lambda, M(z_O)) \cdot T_{Aer}(\lambda, M(z_O)) T_{Ray}(\lambda, M(z_S)) \cdot T_{Aer}(\lambda, M(z_S)) A_{surf}(\lambda, z_O, z_S)}{1 - A_{surf}(\lambda, z_O, z_S) \rho_{Hem}(\lambda, z_O)} \end{aligned} \quad \text{Eq.1}$$

This equation comprises two components: the correction of atmospheric Rayleigh scattering (second line) and the consideration of the surface term (third line), which is affected by the total transmissions of the atmosphere  $T_{Ray}(\lambda; M)$   $T_{Aer}(\lambda; M)$ . This term is calculated by parameterizations for given optical thickness of Rayleigh and aerosol scattering, presented in von Hoyningen-Huene *et al.* (2005). For the L2 data, the Rayleigh path reflectance has already been corrected for, the above equation can be written as:

$$\rho_{Aer}(\lambda) = \rho_{L2}(\lambda) - \frac{T_{Aer}(\lambda, M(z_O)) \cdot T_{Aer}(\lambda, M(z_S)) A_{surf}(\lambda, z_O, z_S)}{1 - A_{surf}(\lambda, z_O, z_S) \rho_{Hem}(\lambda, z_O)} \quad \text{Eq. 3}$$

The equation contains now only the surface term, affected by the total aerosol transmissions  $T_{Aer}(\lambda; M)$ , and hemispheric reflectance of the aerosol contribution  $\rho_{HemAer}$ .

$M(z_s)$  and  $M(z_o)$  are the airmass factors for the satellite and solar zenith distance  $z_s$ ,  $z_o$ , given by Kasten and Young (1989).  $A_{Surf}(\lambda; z_o; z_s)$  is the surface albedo. Considering a Lambert surface the albedo is connected with the surface reflectance  $\rho_{Surf}(\lambda)$  over the cosine of the zenith distances of the illumination and observation angles. Since the calculations of the total transmissions of the aerosol fraction require the unknown AOT, the equation must start with a rough first guess of the AOT and run within an iteration scheme, improving AOT and surface reflectance under constraints for AOT and surface albedo, described later.

$\rho_{Hem}$  is the hemispheric reflection, determined with parameterizations, given in von Hoyningen-Huene *et al.* (2005b), separately for the aerosol contribution  $\rho_{HemAer}$ .

The consideration of the rough estimation of the aerosol contribution is specifically of importance for larger optical thickness greater than 0.5, e.g. desert dust, forest fires or high aerosol pollution. This estimation will be described later in the section of atmospheric correction.

The single steps, which are required to resolve the aerosol reflectance, are described below in detail. An overview of the main procedure for the determination of AOT is given in Figure 7.

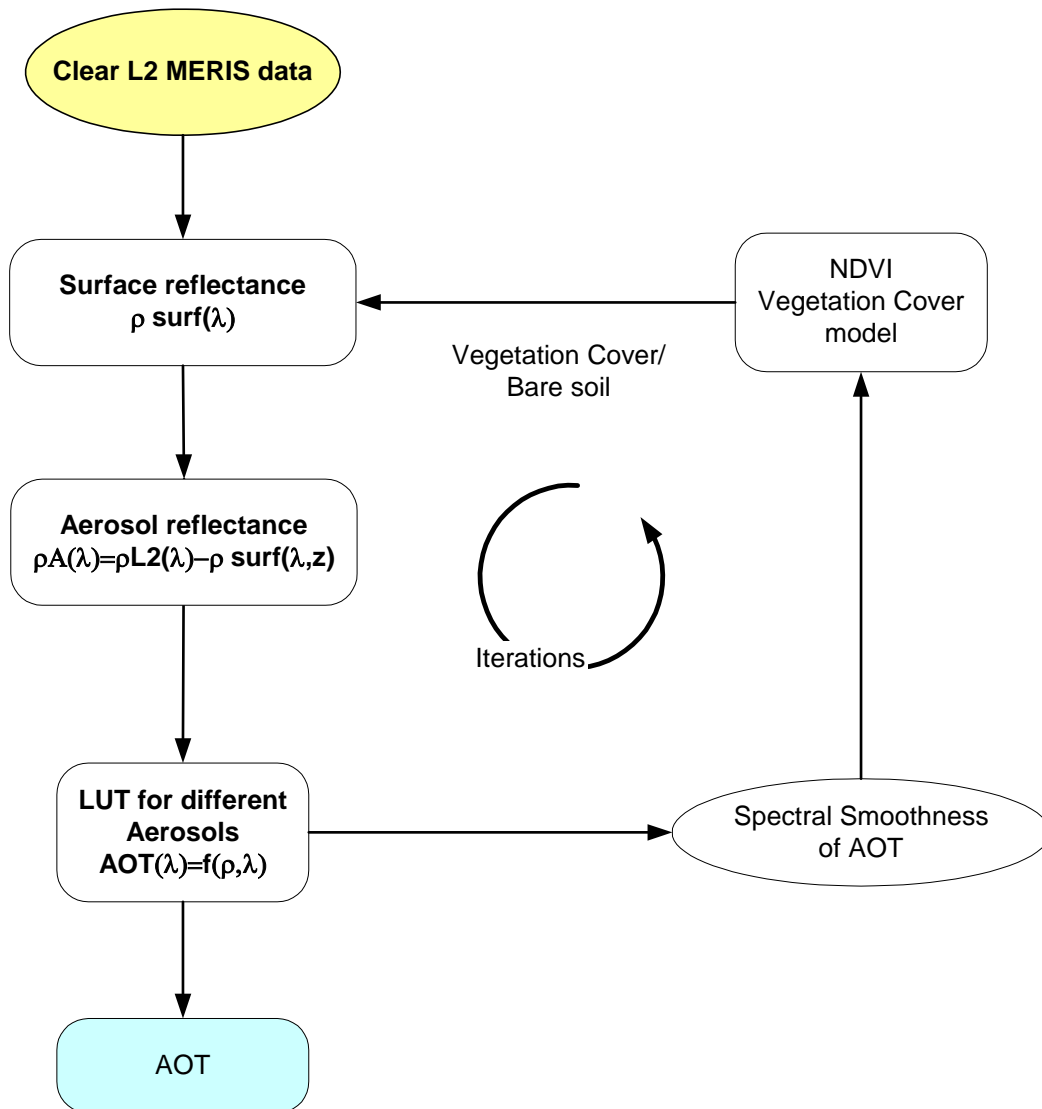


**Figure 7: Scheme of the retrieval procedure for the aerosol optical thickness over land: determination of the aerosol reflectance subtracting the surface reflectance by Eq. 3, described in sections (3.2.2.1) and (3.2.2.3), Application of the LUT and the constraints, described in sections (3.2.2.5) and (3.2.2.3).**

### 3.2.2.2. Separation of Aerosol and Surface Reflectance

The residual value of the TOA-reflectance corrected for Rayleigh scattering reflectance, as provided by the L2 data, contains the common effect of aerosol scattering  $\rho_{Aer}(\lambda)$  and surface reflectance  $\rho_{Surf}(\lambda)$ , (Eq. 3). To separate these parameters, constraints, i.e. additional information, are required and are described in the section of constraints. One needs a relationship, which enables an estimation of the surface reflectance for these channels, where the aerosol retrieval should be made, i.e. in the SW channels lower than  $0.67 \mu\text{m}$ .

BAER estimates the spectral surface reflectance from the satellite scene self, using a spectral surface reflectance model (section 3.2.2.3.1), and constraints to the spectral behaviour of AOT for the 7 short-wave channels of MERIS, for which the AOT retrieval can be made. With Eq. 3, it is finally possible to determinate the aerosol reflectance as a function of wavelength.

#### 3.2.2.2.1 Determination of Total Transmittance and Hemispheric Reflectance

The total transmissions are calculated by the SCIATRAN RTM Rozanov *et al.* (2001) for different values of optical thickness. Using the phase functions for aerosol and Rayleigh scattering and a given range of optical thickness for both scattering processes (aerosols and molecules), down-radiance and up-welling flux has been determined as well as the total transmittance and hemispheric reflectance for different zenith distances. These results have been parameterized into polynomials and used for the retrieval.

Three cases are considered:

- pure Rayleigh atmosphere, using Rayleigh phase function and the optical thickness for Rayleigh scattering for the corresponding wavelength of the channel,
- pure aerosol atmosphere, using an aerosol phase function and a given range of AOT,
- combined effect of both scatterers (aerosol and Rayleigh scattering).

**Table 4: Polynomial coefficients for the determination of the total transmissions**

Coefficient	b0	b1	b2	b3	b4
Rayleigh	-0.44408	+4.49481	-9.71368	+9.49795	-3.42016
Aerosol	+0.01176	+1.01682	-2.32949	+2.11831	-2.32949

**Table 5: Polynomial coefficients for the determination of the hemispheric reflectance**

Coefficient	a1	a2	a3	a4
$\rho_{Hem}$	+0.33185	-0.19653	+0.08935	-0.01674

The Rayleigh scattering part will be needed for the determination of the LUT as described in section 3.2.2.5.

The determination and parameterisations for the total transmissions and hemispheric reflectance used here is from Kokhanovsky *et al.* (2004a).

$$T_{Tot} = \exp\left(-\frac{1}{\cos(z)}\right) \cdot c_{Component}(z) \cdot \delta \quad \text{Eq. 4}$$

The total transmissions are obtained using the optical thickness  $\delta$  and polynomial coefficients  $c_{Component}$ , describing the dependence from the zenith distance:

$$c_{Component}(z) = \sum_{i=0}^4 b_i \cdot \left(\frac{1}{\cos(z)}\right)^i \quad \text{Eq. 5}$$

The  $b_i$  coefficients are different for the different scattering components: i.e. Rayleigh scattering and aerosols, and are given in Table 4.

For the hemispheric reflectance the following polynomial is used:

$$\rho_{Hem} = \sum_{i=1}^4 a_i \cdot \delta^i \quad \text{Eq. 6}$$

The coefficients  $a_i$  are given in Table 5.

For the determination of the total transmittance, the hemispheric reflectance and the atmospheric corrected NDVI, a rough estimation of the aerosol optical thickness,  $AOT_{Guess}$  is required a priori. This first guess of AOT is important for several reasons. It improves the subsequent estimation of the surface properties required for the AOT retrieval, mainly in cases of high aerosol loadings. Studies of heavy dust events like Asian dust events, desert dust outbreaks, forest fire events and heavy anthropogenic pollution have demonstrated that the estimation of both, the NDVI and the hemispheric reflectance are influenced by primarily not known aerosol effects.

### 3.2.2.2 Application of Look-up-Tables and Constraints

The LUTs required in the retrieval process have to be chosen in advance, i.e. the aerosol type must be selected as input parameter before the processing can start. The LUTs are precalculated data in a parameterized form, see section 3.2.2.5. Until now only few aerosol types are available, either derived from closure experiments, or some selected aerosol models from the data base OPAC 3.1 (Optical Properties of Aerosol Components) Hess *et al.* (1998). It contains the aerosol models of the aerosol climatology, given by d'Almeida *et al.* (1991).

The LUT's for the aerosol reflectance  $\rho_{Aer}(\lambda)$  is calculated for a given phase function, single scattering albedo and a range of given AOT and gives the used relationship between aerosol reflectance and AOT. Except in the UV, below 0.4  $\mu\text{m}$  wavelength, the single scattering albedo is typically  $\omega_0 \geq 0.9$ . The largest influence on the aerosol reflectance is determined by the aerosol phase function, which should be appropriate for the aerosol type or types to be retrieved in a selected region. The procedure of generating LUT is described in section 3.2.2.5.

Finally, the application of the constraints, as defined in section 3.2.2.5, in the iterative procedure minimizes the RMSD, the root mean square deviation of the spectral aerosol optical thickness, which has a smooth spectral dependence according to the Angström power law. This procedure yields the aerosol optical thickness at the short-wave MERIS channels 1 - 7 ( $\lambda < 0.665 \mu\text{m}$ ) and an estimate of the Angström turbidity parameters. As a by-product the spectral surface reflectance for the used short-wave channels is also obtained.

The logical procedure, described above, yields the spectral aerosol optical thickness from the aerosol reflectance.



### 3.2.2.3. Constraints Used in the Retrieval of Aerosol Optical Thickness

As mentioned above, to separate aerosol scattering from land surface reflectance, additional information is required, given by the constraints. The constraints used in this method are:

- 1) For the spectral surface reflectance, a linear mixing is assumed between reflectance from vegetation with that of bare soil.
- 2) The wavelength dependence of the aerosol optical thickness is a smooth non-linear function of wavelength defined by the Angstrom power law.
- 3) A weighting parameter to ensure the convergence during iteration.
- 4) Atmospheric correction of used temporary parameters, like NDVI, total transmissions and hemispheric reflectance within the iterative procedure.

These are described in more details as follows.

#### 3.2.2.3.1 Linear Mixing of the Vegetation and Ground Surface Spectral Reflectance

The surface reflectance model, used for the separation of surface effects from atmospheric effects is adapted by two parameters to the conditions within the individual pixel: (a) a linearly mixed spectrum of surface reflectance, composed of spectra of 'green vegetation' and 'bare soil', tuned by the vegetation cover  $C_{Veg}$ , (Eq. 7) and (b) a scaling factor  $F$  to adapt the linearly mixed spectrum to the reflectance conditions within the individual pixel (Eq.8). Both tuning parameters are determined directly from the satellite scene on a pixel by pixel basis.

The linearly mixed spectrum of surface reflectance ( $\rho_{Surf,i=0}(\lambda)$ ) is given by a weighted mixing of spectra from 'green vegetation' and 'bare soil'.

$$\rho_{Surf,i=0}^{Mixing}(\lambda) = C_{Veg} \cdot \rho_{Veg}(\lambda) + SF \cdot (1 - C_{Veg}) \cdot \rho_{Soil}(\lambda) \quad \text{Eq. 7}$$

$C_{Veg}$  represents an estimate of the vegetation cover, estimated from surface NDVI. If  $NDVI \geq 0$ , then  $C_{Veg} = C_{Scal} NDVI$ , where  $C_{Scal}$  is chosen for MERIS with 0.9. If  $NDVI \leq 0$ , the vegetation cover is 0. This assumption is similar to that made by van der Meer and de Jong (2000) for LANDSAT TM data. However, there the fraction of different soil and vegetation types is not derived from the NDVI.

The reference surface spectra used for the mixing are presented in Figure 8.

Both vegetation and ground surface spectral reflectance in the short-wave region ( $\leq 0.5 \mu m$ ) decrease to shorter wavelength. Thus, the effect of surface reflectance decreases to shorter wavelength and the best separation for the aerosol reflectance will be obtained for the lowest wavelength of MERIS.

To adapt the level of the surface reflectance to that required within the satellite scene, a scaling factor  $F$  is introduced.

$$\rho_{Surf}(\lambda) = F \cdot \rho_{Surf,i=0}^{Mixing}(\lambda) \quad \text{Eq. 8}$$

Both tuning parameters are taken from the satellite scene in the following way:

An “atmospherically corrected” NDVI is derived from MERIS channels 13 (0.865  $\mu\text{m}$ ) and 7 (0.665  $\mu\text{m}$ ).

$$NDVI = \frac{(\hat{\rho}(\lambda_{13}) - \rho_{AerGuess}(\lambda_{13}) - \hat{\rho}(\lambda_7) - \rho_{AerGuess}(\lambda_7))}{(\hat{\rho}(\lambda_{13}) - \rho_{AerGuess}(\lambda_{13}) + \hat{\rho}(\lambda_7) - \rho_{AerGuess}(\lambda_7))} \quad \text{Eq. 9}$$

$\hat{\rho}$  is the Rayleigh corrected TOA-reflectance,  $\rho_{AerGuess}(\lambda)$  is determined for a rough estimation of the aerosol optical thickness, obtained from a look-up-table, using a black surface for 0.412  $\mu\text{m}$ , as described in section 3.2.2.4.1.

SF = 1.3 is a constant used to compensate a certain underestimation of the bare soil effect. It is derived from numerous retrievals of spectral AOT.

The scaling factor  $F$  gives the ratio of the surface reflectance for channel 7 (0.665  $\mu\text{m}$ ) obtained (a) from atmospherically corrected reflectance and (b) by the linear mixing model.

$$F = \frac{\hat{\rho}(\lambda_7) - \rho_{AerGuess}(\lambda_7)}{\rho_{Surf}^{Mixing}(\lambda_7)} = \frac{\rho_{Surf}^{AC}(\lambda_7)}{\rho_{Surf}^{Mixing}(\lambda_7)} \quad \text{Eq. 10}$$

Here,  $\rho_{Surf}^{AC}$  (0.665  $\mu\text{m}$ ) is the atmospherically corrected surface reflectance.

The numerator is giving the aerosol reflectance obtained for the channel 1 (0.412  $\mu\text{m}$ ) under the assumption of a black surface; the denominator gives the same from the mixing model. Thus, the spectrum of surface reflectance is adapted to the conditions within the scene.

The transfer of this estimation to the wavelength of 0.665  $\mu\text{m}$  is made by the Angström power law assumption of a spectral slope of  $\alpha = 1.0$ .

The value from the mixing rule  $\rho_{Surf}^{Mixing}$  (0.665  $\mu\text{m}$ ) is taken from Eq 7. This scaling factor contributes much to a stabilization of the solutions and reduces the regional variability over the land surfaces caused by different surface types. At present time, this factor has been determined only for MERIS RR data. It is assumed that a different scaling factor will have to be applied to MERIS FR scenes.

However, few tests with FR data indicate that this factor will only change slightly as compared to RR data.

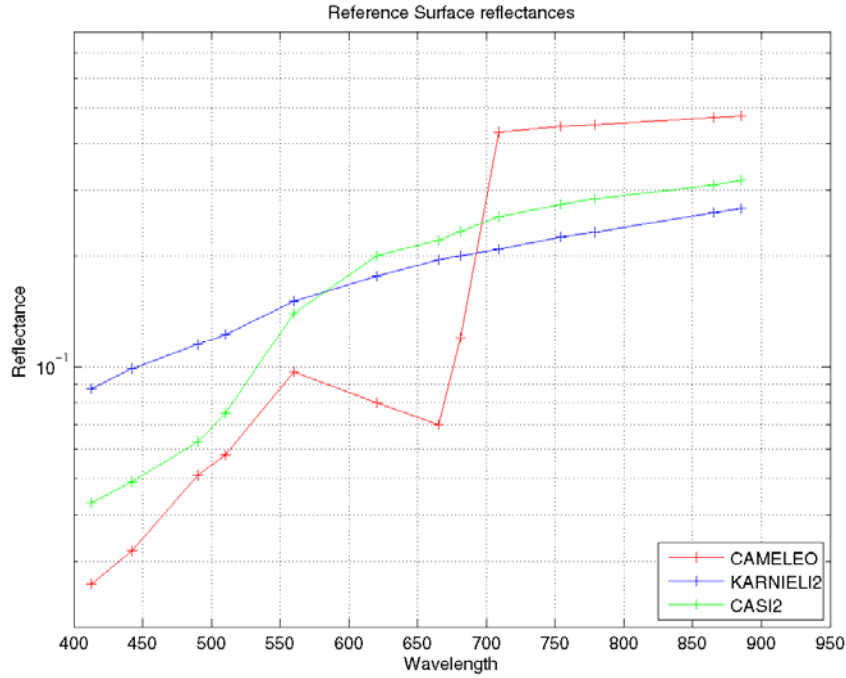


**Figure 8: Spectra used for the determination of the apparent spectral surface reflectance within the BAER approach: The ‘CASI2’ soil spectrum is taken from CASI-radiometer measurements (Olbert (1998)) and the KARNIELI2 desertic spectrum soil is taken from Baret (personal communication). The vegetation spectrum is taken from the CAMELEO database, Escadafal and Bohbot (1999).**

### 3.2.2.3.2 Spectral Behaviour of AOT

The aerosol optical thickness has a smooth spectral behaviour following an Angström powerlaw

$$\bar{\delta}_{Aer}(\lambda) = \beta \cdot \lambda^{-\alpha} \quad \text{Eq. 11}$$

with  $\beta = \delta_{Aer}(\lambda = 1.0\mu\text{m})$ ; the turbidity coefficient and  $\alpha$  the spectral slope.

For this purpose, in contrary to the most two-channel-approaches, c.f. Eck *et al.* (1999), here the Angström parameters  $\alpha$  and  $\beta$  are calculated by the last square fit of the Angström power law with the retrievals for all used spectral channels, i.e. channels 1 to 7 over land.

With this fit, we get:

$$\alpha = \frac{\sum_1^N \left[ \left( \ln \delta_{Aer}(\lambda_i) - \overline{\ln \delta_{Aer}} \right) \cdot \left( \ln \lambda_i - \overline{\ln \lambda} \right) \right]}{\sum_1^N \left[ \left( \ln \lambda_i - \overline{\ln \lambda} \right)^2 \right]} \quad \text{Eq. 12}$$

and

$$\beta = \exp\left(\overline{\ln \delta_{Aer}} + \overline{\ln \lambda} \cdot \alpha\right) \quad \text{Eq. 13}$$

with N - the number of spectral channels used.

$$\overline{\ln \delta_{Aer}} = \frac{1}{N} \sum_1^N \ln \delta_{Aer}(\lambda_i) \quad \text{Eq. 14}$$

and

$$\overline{\ln \lambda} = \frac{1}{N} \sum_1^N \ln(\lambda_i) \quad \text{Eq. 15}$$

describe the averaged logarithms of the spectral AOT and wavelengths, respectively.

This approach gives a much more stable estimation of the Angström parameters than a two-wavelength estimation, especially, if one has errors in the first iterations for the AOT of the single channels.

Further it is easy to transfer the reference wavelength for the AOT from  $\beta = \delta_{Aer}(1.0 \mu\text{m})$  to each wavelength desired. The main purpose of the use of the Angström power law is to ensure the smoothness of the AOT spectrum.

For the first iteration of the determination of the AOT, the surface reflectance obtained by equations 7 and 8 is used. Then, the iterative smoothing described in section 3.2.2.3.3 modifies the spectral surface reflectance.

The Angström parameters are constrained as follows:

The spectral slope  $\alpha$  is determined in the first iteration from the retrieved value of the AOT. It is defined to lie within the limits  $0 \leq \alpha \leq 2.0$ . These boundaries are selected from extreme spectral conditions for the AOT, found in ground-based measurements. If the retrieved spectral slope is outside this limit it is set to the climatologic average of  $\alpha = 1.3$ . This constraint corresponds to the range of the alpha obtained for the majority of atmospheric aerosol types from sunphotometer measurements, Holben *et al.* (2001) and models c.f. d'Almeida *et al.* (1991).

Extensive application of the procedure indicated an insufficient separation of the vegetation peak in channel 5 at  $0.560 \mu\text{m}$ . The vegetation peak at this wavelength is highly variable and this variability is not considered by the linear mixing model of the spectral surface reflectance. This was the reason for increased AOT in this channel and consequently systematic decreased Angström  $\alpha$ .

To reduce this effect the channels are weighted for the determination of Angström  $\alpha$  in different ways. Channel 1 – 4 give the best estimation of AOT, therefore they are used with a double weight for the determination of  $\alpha$ . Channel 5 with this high variability of green vegetation peak is used with the half weight only and channels 6 and 7 with the normal single weight. This weighted use of the 7 MERIS channels lead to a systematic increase of  $\alpha$ . The quite appropriate value of  $\alpha$  is essential for the smoothing, described in section 3.2.2.3.3 and the extrapolation of AOT to channels 8 – 13 for the atmospheric correction of these channels.

The smoothness is estimated from the RMSD determined from the individual estimates  $\delta_{Aer}(\lambda)$  and the value represented by the Angström power law for  $\bar{\delta}_{Aer}(\lambda)$

$$RMSD = \frac{1}{N} \sqrt{\sum_N (\delta_{Aer}(\lambda) - \bar{\delta}_{Aer}(\lambda))^2} \quad \text{Eq. 16}$$

For insufficient smoothness of the spectral aerosol optical thickness, the spectral surface reflectance has to be modified iteratively. Convergence of solution is assumed to have been achieved when  $RMSD \leq 0.005$ .

### 3.2.2.3.3 Iterative Smoothing of AOT

A weighting parameter is introduced to facilitate the convergence in the iterative improvement of the smoothness of the spectral aerosol optical thickness. The aerosol scattering in the blue channel 1 (0.412  $\mu\text{m}$ ) dominates over the land surface reflectance. In addition, atmospheric transmission decreases with wavelength. Thus, the retrieved aerosol optical thickness in this channel has lower relative errors from an inaccurate determination of the surface reflectance. This is expressed in a spectral weighting factor  $\omega(\lambda)$  applied in the iterative modification of surface spectral reflectance.

This factor damps oscillations of the surface spectral reflectance thereby fulfilling the smoothness criterion for the spectral aerosol optical thickness and facilitates a relatively rapid convergence. The weighting parameters have been determined empirically from the set of closure experiments ACE-2 and LACE-98, where all relevant radiative parameters have been measured.

The criterion for the fixing of the weighting factors was the rapid convergence by the individual iteration steps to the known optical thickness from ground-based measurements during the closure experiments. It is fixed with a value of 1.5 for channel 1 (0.412  $\mu\text{m}$ ) and increases to 4.5 for channel 5 (0.560  $\mu\text{m}$ ) or channel 6 and 7 and is used in all cases. A previous version of BAER used smaller values, resulting in increased iteration steps. For the  $i$ -th iteration step  $\rho_{Surf,i}(\lambda)$  is given by :

$$\rho_{Surf,i}(\lambda) = \rho_{Surf,i-1}(\lambda) \cdot \omega(\lambda) \cdot (1 - \Delta_i(\lambda)) \quad \text{Eq. 17}$$

$\omega(\lambda)$  is the mentioned weighting factor taking into account the spectral variability of the surface reflectance and  $\Delta_i(\lambda)$  is the relative deviation of the AOT from the smooth behaviour, defined by the Angström power law term given by:

$$\Delta_i(\lambda) = \frac{(\delta_{Aer}(\lambda) - \bar{\delta}_{Aer}(\lambda))}{\delta_{Aer}(\lambda)} \quad \text{Eq. 18}$$

With this iterative smoothing of the spectral AOT, the spectral surface reflectance is modified, until the RMSD is minimized. The iteration process stops and an output of AOT is made, if  $RMSD < 0.005$  over land. This is the case for about 80% of the cloud free pixels. The remaining cases have less quality and cannot be used for a determination of a reasonable spectral slope of the AOT. There is now one boarder of RMSD enabling an output: 0.005 for all cases with a fast and good convergence of the iterative procedure. In the case of reaching the maximum of iterations and getting a local minimum of RMSD a boarder of  $RMSD < 0.01$  is used to separate between still useful and insufficient results.

The sensitivity of the aerosol reflectance against deviations of the surface reflectance is shown in Figure 9. In the case the iteration lead to the apparent effective surface reflectance of the pixel, the aerosol reflectance can be obtained with an accuracy of 0.005. The adaptation of the apparent

surface reflectance to that situation within the pixel and the minimization of the deviation between the estimation and the real situation is made by three parameters: a) the scaling factor F, adapting the general level of the surface reflectance to radiance level within the scene, b) the atmospheric corrected NDVI, giving the spectral behaviour of the surface reflectance for the short wave channels and c) iterative smoothing of the AOT output, making a fine tuning. Thus, the deviations of the apparent surface reflectance with the existing one should come close to 0. Additionally, the aerosol retrieval is made over areas with fully or partly vegetation cover. There, the expected reflectance for the channels 1 - 7 is in the range of 0.05 and less. Thus, good conditions for the aerosol retrieval exist.

Sensitivity Aerosol Reflectance - Surface Reflectance

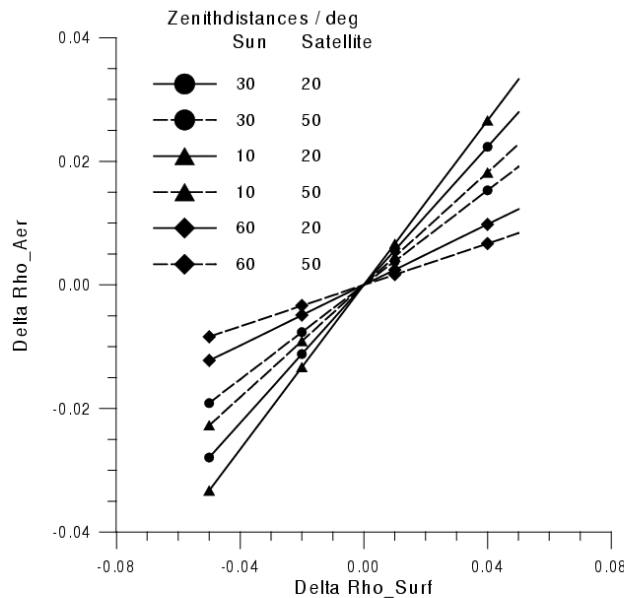


Figure 9: Sensitivity of aerosol reflectance to deviations of the surface reflectance from the correct value

### 3.2.2.4. Atmospheric Correction of Used Parameters Used within the BAER Algorithm

Atmospheric correction is required for a number of parameters used in the BAER algorithm, such as total and direct transmissions, atmospheric reflectance, influencing the total Rayleigh scattering and the NDVI, that is used in the determination of the spectral surface reflectance. Atmospheric correction needs to consider the aerosol effect, which is primarily not known before the processing. Especially, if high aerosol loadings are existent, (strong pollution, dust transports) both the atmospheric transmissions and reflectances are masked significantly by the aerosol itself. Therefore, a first rough estimation of AOT is required at the start of the processing and the aerosol retrieval can only be made in an iterative loop, increasing accuracy from step to step. This was shown by Lee *et al.* (2004) for pollution events during ACE-ASIA.

#### 3.2.2.4.1 Determination of the First Guess Aerosol Effect

For the purpose of the determination of a first guess estimation of AOT in channel 1 ( $\lambda = 0.412 \mu\text{m}$ ), an aerosol optical thickness according to equation 3 is estimated assuming a black surface ( $A_{\text{Surf}} = 0$ ).

Negative spectral slope is assumed with an Angström  $\alpha = 1.0$ .

$$\rho_{\text{AOTguess}}(\lambda) = \rho_{\text{L2}}(\lambda) \quad \text{Eq. 19}$$

and

$$\delta\text{AerGuess} = f(\rho_{\text{AOTguess}}) \quad \text{Eq. 20}$$

$f(\rho_{\text{AOTguess}}(\lambda(1)))$  is the given relationship between  $\delta\text{Aer}$  and the aerosol reflectance  $\rho_{\text{Aer}}$  for the  $0.412 \mu\text{m}$  channel, expressed by the LUT for the given aerosol type.

All LUT's produced for the aerosol reflectance, can be well parameterised with polynomials of second order, starting with  $\rho_{\text{Aer}} = 0$  for an AOT = 0, suitable for a fast processing of the satellite data, see section 3.2.2.5.

Having the first guess for the AOT, the required aerosol transmissions and aerosol reflectance for the atmospheric correction of the used retrieval parameters can be determined, using the look-up-tables (LUT), described in 3.2.2.5.

However, this first guess estimation of AOT gives generally too large AOT, because the effect of surface reflectance is neglected. Therefore, the application of this estimation leads generally to an over-compensation of the atmospheric effect. Consequently, the roughly atmospheric corrected surface reflectance for the channels 7 and 13 at  $0.665$  and  $0.865 \mu\text{m}$ , used for the determination of the NDVI, might be too small. In many cases, this first guess AOT increases the NDVI compared with that obtained without any atmospheric correction, especially in cases of high aerosol loadings. Mainly in these cases, it contributes to an improvement of the apparent surface reflectance and retrieved AOT.

However, in cases with high surface reflectance (sparse vegetation in arid regions, desert ground, and snow cover) this atmospheric correction is the reason for a failing of the retrieval of AOT and needs to be subject of further consideration.

#### 3.2.2.5. **Set-up of Look-up-Tables (LUT)**

The LUTs give the relationships between aerosol reflectance and AOT. They are specific for a certain aerosol type, which should be defined before the retrieval process by the user. At present time, LUTs for three different aerosol types are available: one is derived from experimental investigations during the closure experiment LACE-98, Ansmann *et al.* (2001) and two of them are derived from the OPAC models ('clean continental' and 'average continental', Hess *et al.* (1998).

The relations between  $\rho_{\text{Aer}}$  and AOT are determined with radiative transfer calculations using the radiative transfer code from Nakajima and Tanaka (1988). Similar values as compared to the Nakajima and Tanaka code have been obtained using the RTM GOMETRAN or SCIATRAN, Rozanov *et al.* (1997), Rozanov *et al.* (2001). Aerosol reflectance is strongly dependent on illumination and viewing geometry. Since the RTM includes multiple scattering and exchange between aerosol and Rayleigh scattering, these effects are considered in the LUT.

An ATBD for the ENVISAT radiometer MERIS	Ref	NOV-3341-NT-3352		
	Issue	1	Date	03/11/05
	Rev	0	Date	29/03/06
	Page	40		

### 3.2.2.5.1 Radiative Transfer Calculations for the Generation of LUT

The LUT are generated by calculating the TOA reflectance

$$\rho_{TOA}(\lambda, z_O, z_S, \delta_{Aer}, \delta_{Ray}, p_{Aer}(\theta), p_{Ray}(\theta), \omega_o, A) \quad \text{Eq. 21}$$

for given input parameters  $\lambda$  - wavelength,  $z_O$  and  $z_S$  - zenith distances of sun and viewing geometry,  $\delta_{Aer}$ -AOT,  $\delta_{Ray}$  - Rayleigh optical thickness,  $p_{Aer}(\theta)$  - aerosol phase function,  $p_{Ray}(\theta)$  - Rayleigh phase function,  $\omega_o$  - single scattering albedo,  $A$  - surface albedo (surface reflectance of Lambert ground).

These calculations are made for a whole range of AOT:  $\delta_{Aer} : 0:0...2.5$ . They provide for the given geometry in the first step the relationship between TOA reflectance and AOT for the selected aerosol type.

In a second step, aerosol reflectance is derived from TOA reflectance by equation 1. e.g., it is made in the same manner as it is made by the BAER retrieval, if one would use it with L1b TOA reflectance. Since in these cases, the surface albedo and Rayleigh scattering are known, the separation of  $\rho_{Aer}$  is simple. The calculation of TOA reflectance generally contains the contribution of the exchange between aerosol extinction and Rayleigh scattering. Since the TOA reflectance is now corrected for a pure Rayleigh atmosphere, the obtained relationship between  $\rho_{Aer}$  and AOT, considers the exchange between aerosol extinction and Rayleigh scattering. This is of importance, if highly absorbing aerosol are existent and LUT for such cases should be used. The LUT give the functions linking  $\rho_{Aer}$  and AOT.

### 3.2.2.5.2 Parameters for the Radiative Transfer Calculation

For the radiative transfer computations, three different aerosol phase functions are considered (see Figure 10):

- **Case 1:** Experimental phase function of the LACE-98 closure experiment with increased lateral scattering. It is the average phase function of the period of 8. - 10. August 1998, measured at Lindenberg observatory, south-easterly of Berlin. For these cases, non-spherical particle scattering had to be used, described by the semi-empirical scattering theory of Pollack and Cuzzi (1980). Single scattering albedo in this case is set to  $\omega_o = 0.98$ . The asymmetry parameter  $g$  of the experimental phase function used is found as  $g = 0.55$ . The aerosol data of the LACE-98 experiment are presented in von Hoyningen-Huene *et al.* (2003).
- **Case 2:** Phase function of the 'clean continental' model, obtained with OPAC 3.1 and a single scattering albedo,  $\omega_o = 0.975$ , resulting from the volume mixing ratio of the components of the 'clean continental' aerosol model. The relative humidity was 0.8. The asymmetry parameter of the phase function was  $g = 0.68$
- **Case 3:** Phase function of the 'average continental' model, obtained with OPAC 3.1 and the corresponding single scattering albedo  $\omega_o = 0.928$ . The asymmetry parameter was  $g = 0.70$ .

The scattering angle  $\theta$  is obtained from the zenith distances of illumination and observation  $z_O$  and  $z_S$  and the relative azimuth  $\phi$  between both directions by

$$\cos \theta = -\cos(z_O) \cdot \cos(z_S) + \sin(z_O) \cdot \sin(z_S) \cdot \cos(\phi) \quad \text{Eq. 22}$$





An ATBD for the ENVISAT radiometer MERIS	Ref	NOV-3341-NT-3352		
	Issue	1	Date	03/11/05
	Rev	0	Date	29/03/06
	Page	41		

For the land conditions in all cases of RTM a spectrum of 'green vegetation' is used for the ground albedo, see Fig. 5.

The corresponding LUTs for the three cases are presented in the Figure 11, Figure 12, Figure 13. The presented cases are for  $z_s = 38^\circ$ ,  $z_0 = 23^\circ$  and a relative azimuth  $\Phi = 68^\circ$ . The different curves correspond to the wavelength of the different MERIS channels from 0.412 - 0.885  $\mu\text{m}$ .

The LUT for the channels 1 – 7 are directly required for the retrieval of AOT. The LUT for the channels 8 - 13 will be used for the purpose of atmospheric correction, following up the BAER routine.

One can see from the figures, that the first case gives the lowest AOT for the same aerosol reflectance. It has a phase function with increased lateral scattering, not fitting the assumption of spherical particles, made within the aerosol models. With increasing absorption (decreasing  $\omega_0$ ), the AOT will be increased.

Additionally, the AOT is increased also by the increase of the asymmetry parameter of the phase functions. Phase functions with a higher  $g$  tend to overestimate the AOT. The same is true for decreasing single scattering albedo.

The spread of the LUT for the different channels comes mainly from the varying surface albedo, increasing with the wavelength. In the spectral range of channel 1 - 7, where the surface reflectance is low (over vegetation), up to an AOT of 1.0 the curves are relatively close together.

However, the influence of surface albedo is obvious and shows the need of special data sets for bright ground conditions, like bright bare soils with very sparse vegetation. These are not covered by the approach now. The influence of the surface albedo on the LUT shows also, that approaches, which use a 'black' surface for the aerosol reflectance, as it is made by Kaufman *et al.* (1997a) will be biased by the albedo effect.

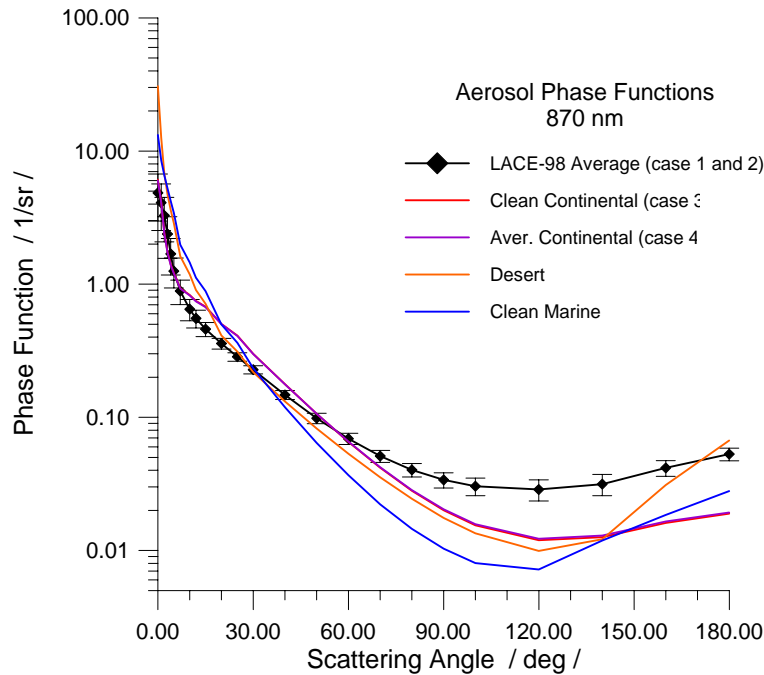


Figure 10: Aerosol phase functions of the cases used for the LUT : (a) experimental phase functions from LACE-98, cases with increased lateral scattering (thick black curves, used in case 1 ), (b) 'average continental' (case 3) and 'clean continental' (case 2) from OPAC. Two more cases are shown in the plot 'desert' from OPAC and 'clean maritime' from OPAC.

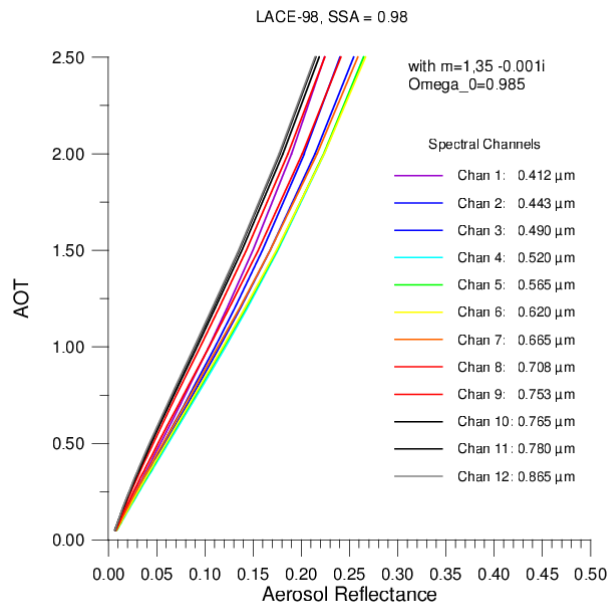
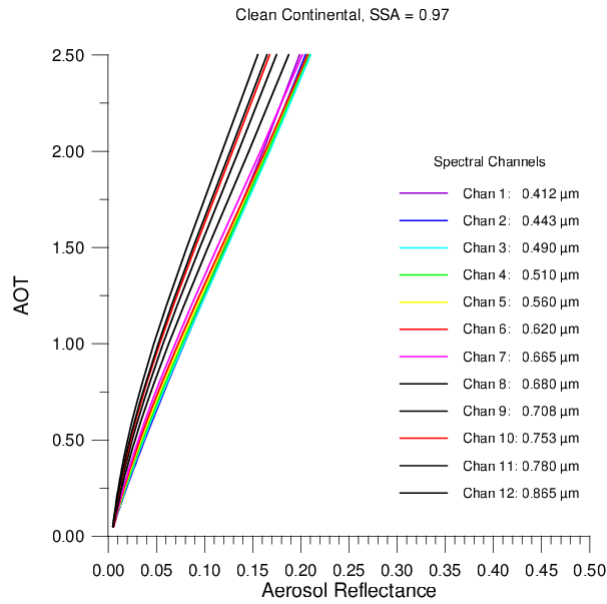
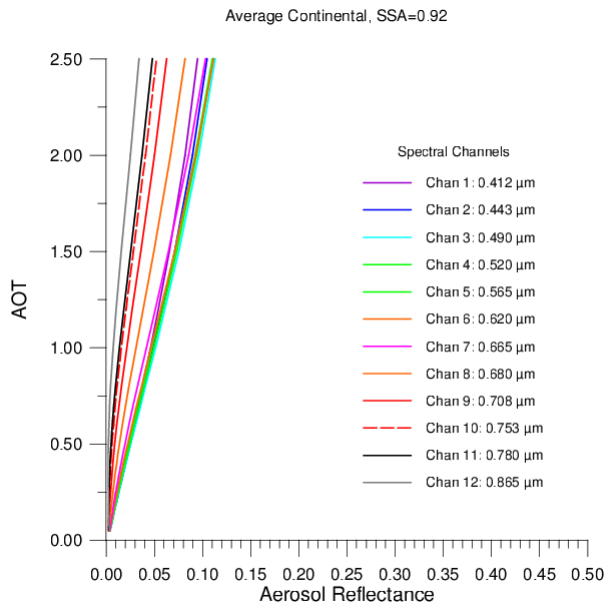


Figure 11: LUT for case 1: LACE-98 aerosol phase function and a single scattering albedo  $\omega_0 = 0.98$ , for land surface conditions for the different channels of MERIS.



**Figure 12: LUT for case 2, using the aerosol phase function and a single scattering albedo  $\omega_0 = 0.975$  of the 'clean continental' aerosol model from OPAC 3.1 Hess *et al.* (1998), for land surface conditions for the different channels of MERIS.**



**Figure 13 LUT for case 3 with an aerosol phase function and a single scattering albedo  $\omega_0 = 0.928$  of the 'average continental' aerosol model from OPAC 3.1 Hess *et al.* (1998), for land surface conditions for the different channels of MERIS.**

### 3.2.2.5.3 Application of LUT within BAER

For a fast application of the curves within the retrieval procedure, the relationships are applied in a parameterized form in terms of polynomials of a second degree, adapted to the LUT from RTM:

$$\delta_{Aer}(\lambda) = A_o(\lambda) + A_1(\lambda) \cdot \rho_{Aer}(\lambda) + A_2(\lambda) \cdot \rho_{Aer}^2(\lambda) \quad \text{Eq. 23}$$

The  $A_i(\lambda)$  are the polynomial coefficients for the single wavelength channels, which are different depending on surface conditions and aerosol type. The equation 23 gives the relationship between  $\rho_{Aer}$  and AOT, called now  $\delta_{Aer} = f_{LUT}(\rho_{Aer})$  for the air mass conditions of the radiative transfer calculations  $M_{z_0}^{LUT}, M_{z_s}^{LUT}$ .

Since these functions for all possible geometries of instrument observation and solar illumination would be required, a fast recalculation to the actual geometry conditions of each pixel is made by using the ratios of air mass factor of calculation and actual conditions:

$$\delta_{Aer}(\lambda) = f_{LUT}(\rho_{Aer}(\lambda)) \cdot \frac{M_{z_0}^{ACT} \cdot M_{z_s}^{ACT}}{M_{z_0}^{LUT} \cdot M_{z_s}^{LUT}} \quad \text{Eq. 24}$$

Thus, for the range of the scan angle  $z_s < 60^\circ$ , like in the case of MERIS and the most conditions of solar elevations, it is possible to use only one parameterisation curve for the retrieval.

Special curves would only be required for cases with low sun elevations, like in the arctic, not used within this BAER approach.

### 3.2.3. **Atmospheric Correction and Determination of Surface Reflectance**

The AOT obtained by the BAER approach, described in section 3.2.2, will be applied in atmospheric correction procedures, considering the aerosol effect for the L2 reflectance data. Two approaches are considered and can be selected by the user (Figure 14):

- (a) the SMAC approach (Simplified Method for the Atmospheric Correction)
- (b) the UBAC approach, an atmospheric correction scheme, associated with the BAER approach (University of Bremen Atmospheric Correction).

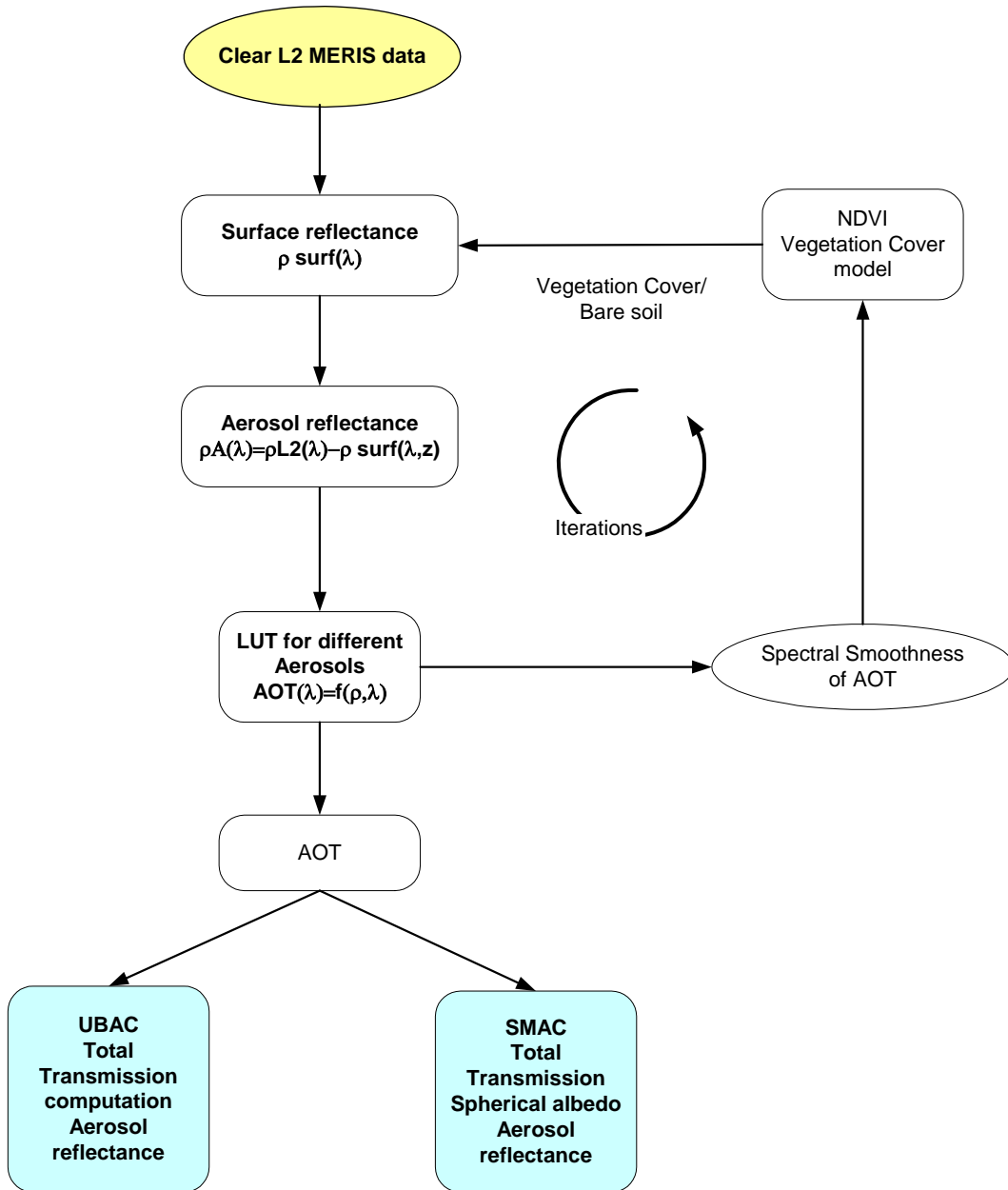


Figure 14: Scheme of the retrieval procedure for the surface reflectances over land.

### 3.2.3.1. Correction of Aerosol Effects by SMAC

The atmospheric correction procedure, developed by Dedieu *et al.*, 1994, updated by Berthelot and Dedieu, 1996 to account for Rayleigh and aerosol multiple scattering and coupling is selected to provide the correction of aerosol effects. In the case of a uniform Lambertian target with reflectance  $\rho_s$ , the reflectance at the top of the atmosphere (TOA),  $\rho_{TOA}$  could be written as.

$$\rho_{TOA} = t_g \cdot \left[ \rho_{R+A} + T(\theta_s)T(\theta_v) \frac{\rho_s}{1 - s\rho_s} \right] \quad \text{Eq. 25}$$

where  $t_g$  is the two-way gases transmittance function,  $T(\theta_s)$  and  $T(\theta_v)$  are total atmospheric scattering transmission (atmospheric transmission normalized by  $T_g$ ),  $s$  is the atmospheric spherical albedo. The term  $\rho_{R+A}$  denotes contribution from Rayleigh and aerosol scattering over non-reflecting surface.

The atmospheric correction scheme for a non aerosol corrected image consists in the inversion of the following equation where SMAC Rayleigh correction is removed from the processing by setting the Rayleigh terms to 0.

SMAC method allows to estimate surface reflectance from Top Of Aerosol reflectances (MERIS Level 2) and the knowledge of the state of the atmosphere (aerosol contents). The scattering process is parameterized by analytical formulations whose coefficients, which are depending on the spectral bandwidth of the sensor, are fitted against the 6S radiative transfer reference code (version 4.1). Improvements fall on the best taking into account of multiple scattering and the coupling between aerosols and molecule, and the taking into account of the altitude of the target. It is able to fulfil the specifications of the project in terms of operationality and accuracy.

The inputs of SMAC are the AOT of 0.55  $\mu\text{m}$ , and geometry acquisition (sun and view zenith angle, relative azimuth angle). The aerosol correction is performed using a continental aerosol type. The AOT of 0.55  $\mu\text{m}$  is taken from the BAER retrieval (extrapolated using the angstrom power law from AOT in channel 1 and angstrom coefficient). It is applied on a pixel-by-pixel basis (if AOT is available).

$$\delta_{Aer}(\lambda = 550\text{nm}) = \delta_{Aer}(\lambda = 412\text{nm}) \cdot \left[ \frac{\lambda = 550\text{nm}}{\lambda = 412\text{nm}} \right]^{-\alpha} \quad \text{Eq. 26}$$

### 3.2.3.2. Correction of Aerosol Effects by UBAC

With the knowledge of the AOT, which has already been computed within BAER, the relationships between AOT and aerosol reflectance, the total transmissions and air mass factors, the atmospheric correction can be performed resolving equation 3 for the albedo (surface reflectance in the case of a Lambert ground).

$$A_{Surf}(\lambda) = \frac{(\rho_{L2}(\lambda, zO, zS) - \rho_{Aer}(\lambda, zO, zS))}{T_{Aer}(\lambda, Ms) \cdot T_{Aer}(\lambda, Mo)} \cdot (1 - A_{Surf}(\lambda, zO, zS) \cdot \rho_{Hem_{Aer}}(\lambda, zO)) \quad \text{Eq. 27}$$

The last term in equation 27 can be neglected for most cases, because in the most cases it is close to 1. Except in the case of very bright grounds, where this assumption leads to a slight underestimation of the surface reflectance.

Ref	NOV-3341-NT-3352		
Issue	1	Date	03/11/05
Rev	0	Date	29/03/06
Page	47		

With equation 27, the atmospheric correction can be performed, the final output of this processing is the spectral surface reflectance. Since the AOT is given by BAER only for the channels 1 - 7, the AOT for the channels 8 - 13 is determined by the Angström powerlaw,

$$\delta_{Aer}(\lambda) = \delta_{Aer}(\lambda = 412nm) \cdot \left[ \frac{\lambda}{\lambda = 412nm} \right]^{-\alpha} \quad \text{Eq. 28}$$

At this point, BAER has estimated the AOT in 13 MERIS bands. This information is now used for the computation of the aerosol reflectance, which is obtained from the solution of the polynomial fits for the LUT, see section 3.2.2.5.

In a last step, aerosol reflectance for all MERIS channels is used in equation 27 and the atmospheric corrected surface reflectance is obtained in all 13 MERIS channels. This surface reflectance is related to an isotropically reflecting flat Lambert surface. Effects of bi-directional anisotropy and surface tilt are not considered.

## 4. Results and Conclusion

---

### 4.1. Results of the approach

This section will give a short overview of the result obtained using the full Integrated BAER method. Detailed information on results and their validation are given in the separate validation report, BAER validation report, 2006.

Within this project, the BAER approach has been applied in different regions. The main results are:

- b. The spectral AOT, retrieved from MERIS channel 1 – 7,
- c. The Angström  $\alpha$  parameter,
- d. The extrapolated AOT for MERIS channels 8 – 10 and 12 – 14,
- e. The atmospheric corrected surface reflectance for channels 1 – 10, 12-14.

Within this section, only exemplarily results of BAER for one example will be shown, demonstrating the capabilities and the retrieved physical aerosol and surface parameter by the procedure

As one example for the application to L2 data, a scene from Spain 13. April 2003, MER\_RR\_20030413\_101045 L2, is shown (Figure 15). The LUT of case 1 (LACE-98) is used. The AOT is obtained over the most regions of Spain, except where dry bright regions are existing, e.g. few regions in the centre of Spain and the Sahara region. There, the surface reflectance is too large and does not fit with the conditions of the present BAER version. The first guess AOT leads to wrong estimations for the surface reflectance, not supporting the iterative procedure.

For the other parts of the scene, the AOT seems to be given in the right range, unless for this scene only 2 AERONET instruments had data and not exactly to the overflight time (Table 6)

Spectral AOT, retrieved from the MERIS RR scene, over southern France and Spain of the 13. April 2003 are presented in Figure 16. The retrieved part of the spectra is indicated and the extrapolated continues the retrieved section to all MERIS channels. The presented spectra show different types, which have been found within the scene.

One type is found as 'normal aerosol' with the expected spectral slope and decreasing AOT with increasing wavelength. As one can see in the double logarithmic presentation, the spectral follows nearly an Angström power law, with deviations in the channels 1 and 2. There a slight weakening of the spectral decrease can be observed.

A second type is found with flat or neutral spectra. One group with low AOT could be connected with marine aerosols, because the spectra have been selected close to the Atlantic coast northerly of the Pyrenees.

Another group of spectra is also connected with flat spectral slopes, however with an increased AOT. These spectral could be connected with disturbances of thin cirrus clouds.



Spectra of the surface reflectance picked from several places of the scene are shown in Figure 17. The spectra are picked to demonstrate the different surface types. The atmospheric correction leads to the expected general decrease of the surface reflectance to shorter wavelength. One can distinguish between different vegetation types, different degree of vegetation cover and bare soil.

**Table 6: Ground-based and retrieved AOT of the scene of the 13. April 2003 over southern France and Spain**

Location	AOT retrieved	AOT AERONET
Toulouse	0.186	0.167
Avignon	0.250	0.249

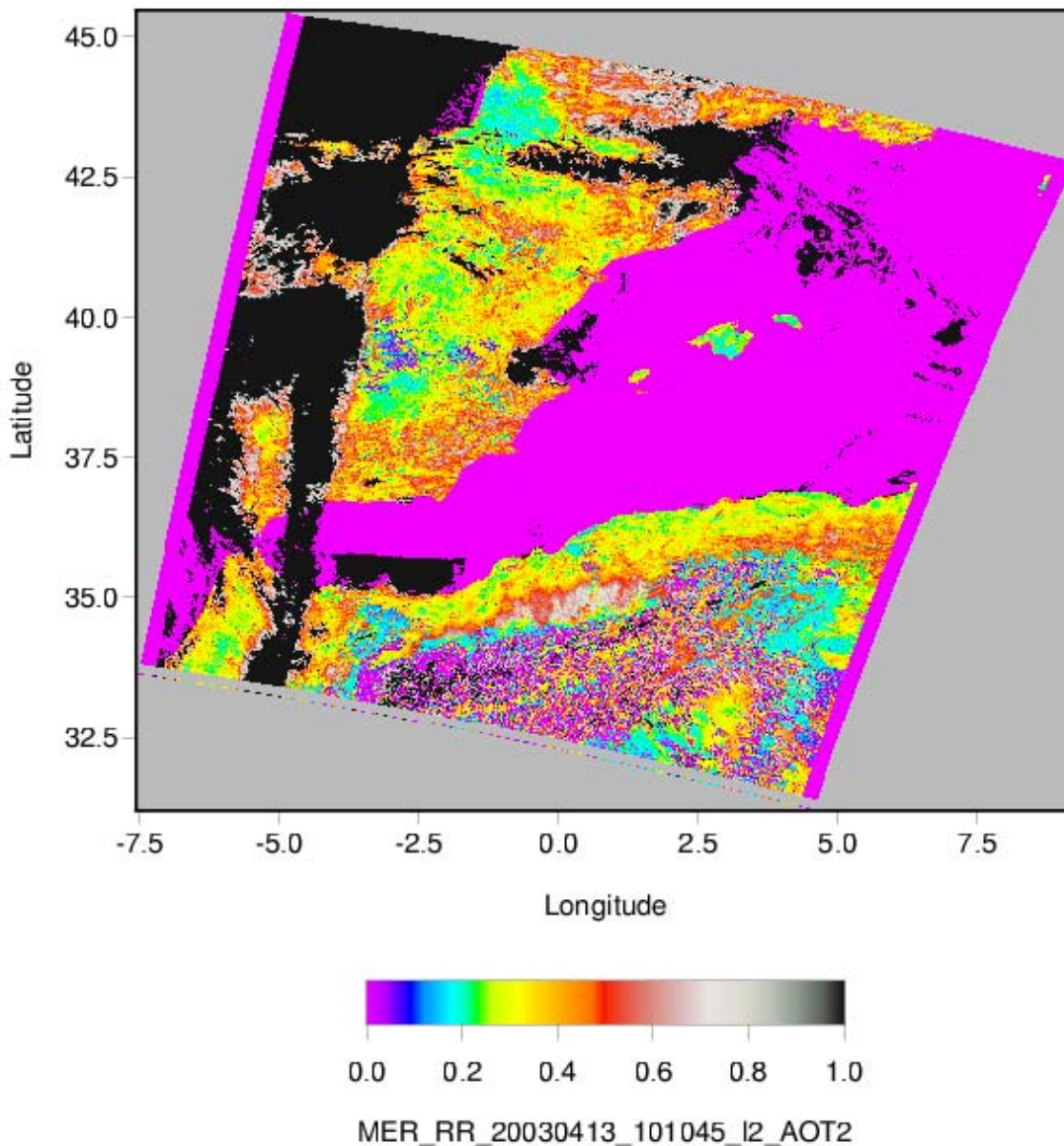


**Figure 15: Aerosol optical thickness for channel 2 (0.443  $\mu\text{m}$ ) over Spain from MERIS L2 data, taken at 13. April 2003, 10:10:45.**

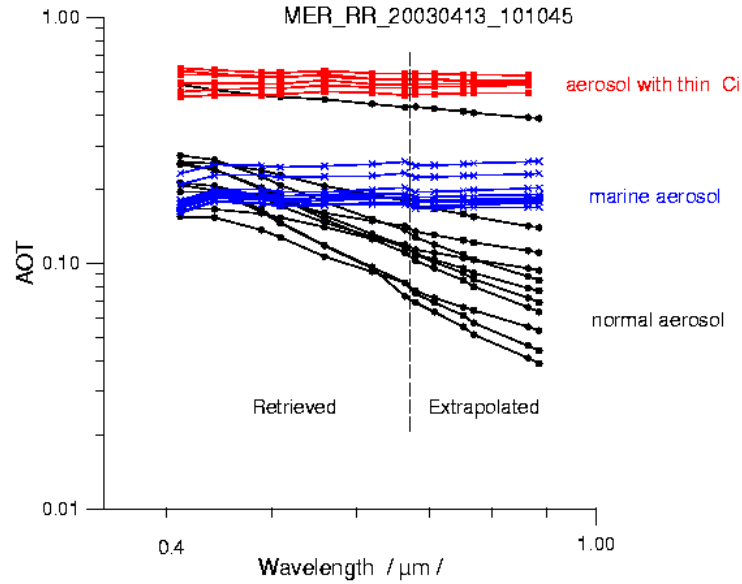


**Figure 16: Composition of different spectral AOT, retrieved from the scene over France and Spain from MERIS L2 data for the 13. April 2003.**

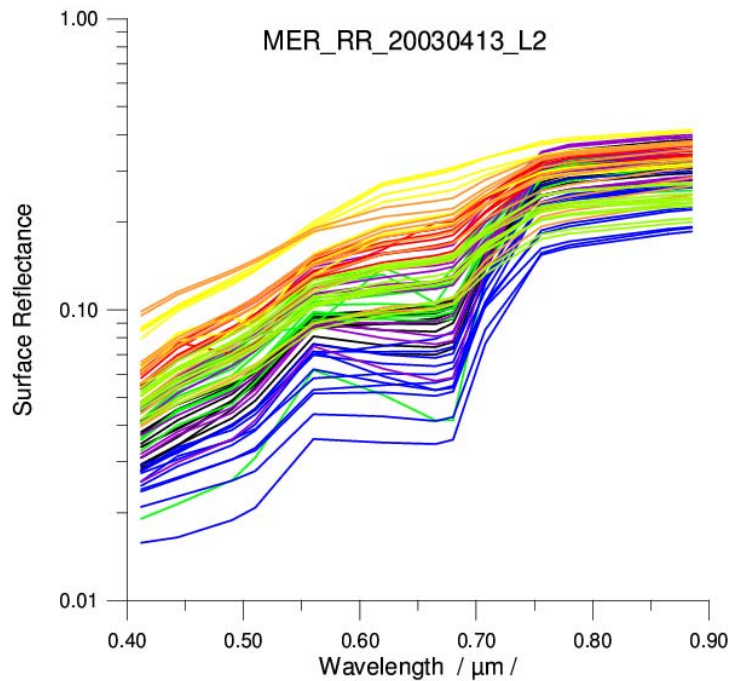


**Figure 17: Spectral surface reflectance of different places within the scene over Spain from MERIS L2 data for the 13. April 2003.**

## 4.2. Validation Plan

The adaptation and preparation of this algorithm for the application with MERIS data required an inter-active validation and modification of parameters within the algorithms until they can fix for the MERIS application. This task required coincident MERIS overflights with ground-based data, especially on aerosol optical thickness to compare the retrieval results with ground-based data on aerosol optical thickness. Disagreements lead to modifications and improvements within the retrieval procedure, especially in the estimation of the apparent surface reflectance for the MERIS channels, until coincident results for the AOT had been obtained. This task is mainly done and will be described within the validation report, c.f. BAER validation report, 2006.

Regions with multiple operational sunphotometers will be used, that multiple ground-based measurements can be found in one scene. Most of the instruments are operated by the AERONET, however access to data from instruments operated by the DWD and KNMI is available. Especially validation regions are: France with approximately 9 instruments, Italy 6, Northern Germany and Netherlands 6, Southern Germany 2, Spain 2, Poland 2 and some single instruments in the region of the Baltic Sea and Eastern Europe. A good validation region outside of Europe is the eastern coast of the US, because multiple AERONET instruments are there in operation.

An additional validation is the comparison of the MERIS retrieval of the AOT with the retrievals using MERIS official products obtained by Santer *et al.*, 2000 (AOT at 865 nm and angstrom coefficient) and the MODIS Atmosphere products both for Terra and Aqua (AOT and angstrom coefficient).

## 4.3. Conclusion, Outlook

The present state of the development of BAER using MERIS L2- data gives quiet sufficient results for regions like Europe. These are regions, where a certain fraction of cover with green vegetation exists and the variation of the surface reflectance, caused by bare soil fractions are not dominant.

All parameters in the program are now fixed in such a way, that for Europe comparable results with BAER retrievals and ground-based AOT are obtained. Even for larger pollution quite acceptable AOT could be obtained. Thus for Europe the retrieved AOT for the SW channels of MERIS, using LUT of case 1 is within a range of 25%, compared with ground-based measurements. For the channel 7, 665  $\mu\text{m}$  the agreement is found with 35%.

3 cases of LUT are provided, derived from experimental aerosol parameters and from continental aerosol models. The best results for the AOT retrieval in Europe are obtained with experimental aerosol parameters obtained during the LACE-98 experiment. For the one case of a scene over China, however, this LUT leads to a significant underestimation of the AOT (of about 30%).

The present data base of LUT is still restricted to the three types. The validity of the LUT for specific regions is an open issue, because the user needs some recommendations for his selection. This must be subject of a validation in different regions of the world. The data base of available LUT should be extended. There are missing LUTs, describing the properties for marine aerosol, for desert conditions, biomass burning and others.

Atmospheric corrected spectra of surface reflectance with all MERIS channels are obtained. They allow the recognition of different surface types, different vegetation, different vegetation cover, bare soil conditions. Since the focus of this part of the project was on the retrieval of a quite correct AOT, a deeper validation of the obtained surface parameters is required.



Ref	NOV-3341-NT-3352		
Issue	1	Date	03/11/05
Rev	0	Date	29/03/06
Page	52		

The most applications have been made with reduced resolution data. The application with full resolution data is also possible. Modifications within the surface reflectance model seem to be not required, because a reliable AOT for the SW channels (channel 1 and 2) could be obtained. An extended application and validation of BAER, using full resolution data is required. Effects of the use of FR data on the spectral behaviour of the AOT and their extrapolation to the NIR channels are not yet investigated.

Investigations of the validity of the used model for the apparent spectral surface reflectance in other regions of the world have to be made. The present applications mainly have been restricted to conditions of Europe. Possible variations of different vegetation types and their influence on the spectral AOT, such as tropical ones or boreal forests have not been tested. The same is valid also for different bare soil conditions. The result of such investigations should decide on the acceptance of the present surface reflectance model or its extension with more basic types of different vegetation spectra and bare soil spectra.

Clearly improvements are required for brighter surfaces, as well for specific LUT, as well for the first guess AOT to get a reliable estimation of the initial surface reflectance for the retrieval procedure.

Presently inland water areas (lakes) are in the approach, using L2 data are more or less generally excluded, because the atmospheric correction for water surfaces including a wrong aerosol correction will be applied by the regular L2 processor. Thus BAER in this specific version for L2 data cannot be used, because inland water areas are not processed as other land surfaces. A modification of the approach for atmospheric correction using BAER also with MERIS L1 data would overcome this problem. This would give homogeneous datasets of AOT over land and water areas, enabling the atmospheric correction also over inland water. It also enables the investigation of the AOT pattern over both land and ocean.

Since the BAER method also enables the determination of spectral behaviour of the AOT, especially of Angström, future extensions are possible, as there are:

- ◆ estimation of aerosol type from the retrieved spectral aerosol optical thickness and reprocessing with a specific coefficient set for the specific aerosol type. This requires a selection of relevant aerosol types for the retrieval, their discrimination, the preparation of look-up-tables for the types and their application.
- ◆ using size distribution models to estimate effective radius and aerosol number or volume concentration, which can be helpful for the derivation of other aerosol pollution parameters.

Especially these future extensions can provide new applications in environmental pollution control, health care, aerosol - cloud interactions and much other.

Finally, from the present status of the method development it can be concluded, that BAER is a powerful tool for aerosol investigation from space, using MERIS and for atmospheric correction.



Ref	NOV-3341-NT-3352		
Issue	1	Date	03/11/05
Rev	0	Date	29/03/06
Page	53		

## 5. Assumptions and limitations

---

### 5.1. Assumptions

#### 5.1.1. Aerosol optical thickness estimation

The retrieval in case of heavy aerosol loading is not validated. The impact of subpixels cloud pollution provided false AOT estimation.

#### 5.1.2. Surface reflectance estimation

- UBAC Surface reflectances

The last term in equation 27 which is neglected can lead in the case of very bright grounds, a slight underestimation of the surface reflectance.

- SMAC surface reflectances

The parameterisation of SMAC is based on the continental aerosol model, whereas aerosol estimated using BAER are different.

### 5.2. Limitations

- The BAER algorithm is limited and can not be applied over bright ground surfaces where the AOT values might be overestimated.
- The surface reflectance is related in both methods to an isotropically reflecting flat Lambert surface. Effects of bi-directional anisotropy and surface tilt are not considered.



Ref	NOV-3341-NT-3352		
Issue	1	Date	03/11/05
Rev	0	Date	29/03/06
Page	54		

## 6. Practical considerations

---

### 6.1. Integrator processor user's guide

The integrated BAER processor (IBAER) is a complete tool for performing aerosol optical thickness and surface reflectance retrieval over land. BAER integrated processor handles Level 2 MERIS data in full and reduced resolution. The interface has been designed to allow the user the choice of input data, and processing options.

The user interacts with IBAER processor through a graphical user interface. The aspect of the usage of IBAER processor are summarised in the next sub sections. The user manages the data generated by the software. Technical description of the Integrated BAER processor can be found in the Detail Processing model document, referred by NOV-3341-NT-3711.doc.

The subsections will guide the user through the three steps of Integrated BAER processor.

#### 6.1.1. Software and hardware requirement

The Integrated BAER processor has been developed in Java code, to be integrated into the BEAM toolbox (BEAM, 2004)<sup>1</sup>.

#### 6.1.2. Integrated BAER processor Set Up

The set up and plug in of the BAER Integrated processor is:

1. Download and unzip the plug-in \*.zip archive. It will contain a \*.jar file, which is the actual plug-in, and in most cases a `readme.txt` file. Some plug-ins also come with source code which is then stored in a sub-directory called `src` by convention. A plug-in may also require extra auxiliary data (e.g. data processors) to perform well. This is usually stored in a sub-directory called `auxdata` by convention.
2. If not otherwise stated in the `readme.txt`, a plug-in is usually installed by copying the \*.jar file into the `extensions` sub-directory of your BEAM installation directory.
3. If the `auxdata` sub-directory exists in the \*.zip archive, copy its content into the `auxdata` sub-directory of your BEAM installation directory.

All BEAM plug-ins have to be re-installed if you install a new BEAM version on your computer.

---

<sup>1</sup>BEAM is the Basic ERS & Envisat (A)ATSR and Meris Toolbox and is a collection of executable tools and an application programming interface (API) which have been developed to facilitate the utilisation, viewing and processing of ESA MERIS, (A)ATSR and ASAR data. Please refer to the BEAM web site for BEAM installation.

### 6.1.3. Overview of the user interface

Figure 18 gives an overview of the BAER Integrated processor user interface. Two panels are available. The first one is dedicated to the choice the input /output data and written format. The second is dedicated to the choice of retrieval parameter.



**Figure 18: Integrated Baer processor panels**

The first panel controls the 3 fields. They are:

- Field 1: The selection of the input data
- Field 2: The selection of the output data location and filename
- Field 3: The selection of output product format

The second panel controls the 3 buttons and three fields necessary to perform the parameter retrieval. They are:

- Button 1: Control of the activation of the cloud screening method
- Button 2: Control of the activation of the aerosol parameter computation
- Button 3: Control of the activation of the atmospheric correction method used
- Field 4: The selection of the atmospheric method among SMAC or UBAC
- Field 5: The choice of the aerosol LUT (OPAC\_CC, OPAC\_AC, LACE98)
- Field 6: The choice of input bitmask applied to the image.

### 6.1.4. Data management

Input and Output data are managed by the user through the interface.

### 6.1.5. Option activation

#### 6.1.5.1. The cloud screening option

This option is always active. The algorithm is described in section 3.2.1.



Ref	NOV-3341-NT-3352		
Issue	1	Date	03/11/05
Rev	0	Date	29/03/06
Page	56		

### 6.1.5.2. The AOT and angstrom exponent computation selection

The activation of the option allows the user to compute the atmospheric parameters which are the Aerosol optical thickness and the aerosol angstrom coefficient.

When activated, the user selects the Aerosol Look Up Table which will be used as reference in the processing. Three LUT are available for the retrieval. Based on a a priori knowledge of the aerosol type to retrieve, the user can select one of the three LUT. In the other cases, it is recommended to use the LACE 98 LUT.

### 6.1.5.3. The surface reflectance computation selection

If the previous step is active, the user can compute the surface reflectances in the thirteen MERIS channels. Two methods are then proposed, SMAC and UBAC. The user addresses its choice by clicking the method panel.

## 6.2. Integrated processor Input/Output

### 6.2.1. Input data

Standard MERIS L2 products are used in both full and reduced resolutions. These products are called “top-of-aerosol” reflectance, which is the top-of-atmosphere reflectance corrected for the Rayleigh path reflectance and all gaseous absorptions, O<sub>3</sub> and, H<sub>2</sub>O vapour, (Santer, 2000).

The used Level 2 data are  $\rho_{L2}$  are the Norm. rho\_surf - MDS (\*) data sets.

### 6.2.2. Output data

The number of output depends on the number of options selected by the user. The number of output channel is 1 if only the cloud mask is computed, 5 if the AOT are computed, 21 if the surface reflectances are computed.

#### 6.2.2.1. Cloud channel

A cloud mask is created as output of the processing. The cloud mask contains three states, which are:

0 = Clear

1 = Cloud detection using BAER function

2 = Cloud detection issue copied from Level 2 MERIS data flag channel

The mask is coded in int.

#### 6.2.2.2. Atmosphere products

The BAER algorithm generates four channels

- The Aerosol Optical Thickness at 412 nm
- The Aerosol Optical Thickness at 440 nm
- The Aerosol Optical Thickness at 550 nm





Ref	NOV-3341-NT-3352		
Issue	1	Date	03/11/05
Rev	0	Date	29/03/06
Page	57		

- The angstrom exponent

These outputs are coded in float.

### 6.2.2.3. Surface reflectance products

The surface reflectances in the thirteen channels are created as output. In addition, the “toa\_veg<sup>2</sup>” channel (Gobron *et al.*, 2000) is recopied from the input data to allow user interested by vegetation products to use this channel.

These outputs are coded in float.

### 6.2.3. Naming convention

The naming convention for Integrated BAER products is:

- **CLOUD** for the cloud channel
- **ALPHA** for the angstrom exponent
- **AOT\_412** for the aerosol optical thickness in MERIS channel 1
- **AOT\_440** for the aerosol optical thickness in MERIS channel 2
- **AOT\_550** for the aerosol optical thickness in MERIS channel 5
- **reflec\_1** for the surface reflectance in MERIS channel 1
- **reflec\_2** for the surface reflectance in MERIS channel 2
- **reflec\_3** for the surface reflectance in MERIS channel 3
- **reflec\_4** for the surface reflectance in MERIS channel 4
- **reflec\_5** for the surface reflectance in MERIS channel 5
- **reflec\_6** for the surface reflectance in MERIS channel 6
- **reflec\_7** for the surface reflectance in MERIS channel 7
- **reflec\_8** for the surface reflectance in MERIS channel 8
- **reflec\_9** for the surface reflectance in MERIS channel 9
- **reflec\_10** for the surface reflectance in MERIS channel 10
- **reflec\_12** for the surface reflectance in MERIS channel 12
- **reflec\_13** for the surface reflectance in MERIS channel 13
- **reflec\_14** for the surface reflectance in MERIS channel 14
- **BAER\_FLAGS** for the flag channel associated to the processing

---

<sup>2</sup>Toa\_veg is also named by Fapar or MGVI



An ATBD for the ENVISAT radiometer MERIS	Ref	NOV-3341-NT-3352		
	Issue	1	Date	03/11/05
	Rev	0	Date	29/03/06
	Page	58		

### 6.2.3.1. Quality control and diagnostics

Flags are generated during the processing to allow the user to interpret the results. Seven 1 bit flags are generated. The default value is false, which represents valid value. The following describes error or exception conditions, which are flagged by setting the corresponding bit to true:

- **Bit 1:** The flag `INVALID` is set to true if **any** error condition evaluates to “true” and raises a specific error flag.
- **Bit 2:** The flag `INVALID_INPUT` is set to “true” if any one of the input measurement data has a value  $\leq 0.0$  or if the input pixel was skipped due to input flagging. Error condition raises also `INVALID` flag.
- **Bit 3:** The flag `CLOUD_INPUT` is set to “true” if the pixel is cloudy.
- **Bit 4:** The flag `AOT_OUT_OF_RANGE` is set to “true” if the calculated AOT is out of the valid range [0.02-2]. Error condition raises also `INVALID_OUTPUT` flag.
- **Bit 5:** The flag `ALPHA_OUT_OF_RANGE` is set to “true” if the calculated ALPHA coefficient is out of the valid range [0-2]. Error condition raises also `INVALID_OUTPUT` flag.
- **Bit 6:** The flag `INVALID_OUTPUT` is set to “true” if the calculated surface reflectance is superior to 1.0 or negative in at least one spectral band.
- **Bit 7:** The flag `SMAC_CORRECTION` is to “true” if the SMAC atmospheric correction is used. It is set to false if the UBAC method is used.

If only the AOT and cloud processor are activated, the bit 6 and 7 are set to false.

## 7. References

---

- Ansmann, A., Wandinger, U., Wiedensohler, A., Leiterer, U., 2001.** Lindenberg aerosol characterization experiment 1998 (LACE 98): Overview. *J. Geoph. Res.*, 107 D21.
- Antoine, A., Morel, A., 2000.** MERIS ATBD 2.7 : Algorithm theoretical basis document, atmospheric correction over the ocean (case 1 waters). Technical report PO-TN-MEL-GS-0005, LPCM.
- ASCAR, 2003.** Algorithm survey and critical analysis report. report to ESA ESRIN. Technical report NOV-3160-NT-1442v2, ASCAR.
- BAER Input/Output Data Document**, Berthelot, B., Castillon C., 2006 (NOV-3341-NT-3711).
- BAER DPM Document**, Berthelot, B., Castillon C., 2006 (NOV-3341-NT-3712).
- BAER Validation Report, 2006.** von Hoyningen-Huene, B. Berthelot, W., Kokhanovsky, A., Burrows, J.P.: Validation report of Integrated BAER processor applied to MERIS L2 data. (NOV-3341-NT-3284.pdf)
- BEAM, 2004.** Beam web-page. URL <http://envisat.esa.int/services/beam/>.
- Berk A., G. P. Anderson, P. K. Acharya, J. H. Chetwynd, L. S. Bernstein, E. P. Shettle, M. W. Matthew, and S. M. Adler-Golden, 2001:** MODTRAN4 Version 2 User's Manual, p. 98. Air Force Research Laboratory. Space Vehicles Directorate. Air Force Material Command. Hanscom AFB, Massachusetts.
- Berthelot, B., Dedieu, G., 1997.** Correction of atmospheric effects for VEGETATION data. Physical Measurements and Signatures in Remote Sensing, Guyot & Phulpin (eds), Balkema, Rotterdam, ISBN 90 5410 9173
- Bezy, J.-L., Delwart, S., Rast, M., 2000.** Meris - a new generation of ocean colour sensor onboard Envisat. Technical report EAS Bulletin 103 (2000) 48-56, ESA.
- Bhartia, P. K., Herman, J. R., Ahmed, Z., Gleason, J., 1998.** Derivation of aerosol properties from satellite measurements of backscattered ultraviolet radiation : Theoretical basis. *J. Geoph. Res.*, 103, 17.099–17110.
- d'Almeida, G. A., Koepke, P., Shettle, E. P., 1991.** *Global climatology and radiative characteristics*. Deepak, Hampton. 561 pages.
- Dedieu, G. et al., 1994.** SMAC: A simplified method of atmospheric correction of satellite measurements in the solar spectrum. *Int. J. Remote Sensing*, 15, 123-143.
- Deuzé, J.-L., Herman, M., Goloub, P., Tanré, D., Marchand, A., 1999.** Characterization of aerosol over ocean from POLDER/ADEOS-1. *Geoph. Res. Letters*, 26, 1421–1424.
- Eck, T. F., Holben, B. N., Reid, J. S., Dubovik, O., Smirnov, A., O'Neill, N. T., Slutsker, I., Kinne, S., 1999.** Wavelength dependence of the optical depth of biomass burning, urban and desert dust aerosols. *J. Geoph. Res.*, 104, 31.333–31.349.

- Escadafal, R., Bohbot, H., 1999.** Changes in arid mediterranean ecosystems on the long term and earth observation. Technical report, Annual Report 1999, CAMELEO Project. URL <http://www.egeo.sai.jrc.it/cameleo/index.html>.
- Geogdzhayev, I. V., Mishchenko, M. I., Rossow, W. B., Cairns, B., Lacis, A. A., 2002.** Global two-channels AVHRR retrievals of aerosol properties over oceans for the period of NOAA-9 observations and preliminary retrievals using NOAA-7 and NOAA-11 data. *J. Atmos. Sci.*, 59, 262–278.
- Goloub, P., Tanré, D., Deuzé, J.-L., Herman, M., Marchand, A., Bréon, F.-M., 1999.** Validation of the first algorithm applied for the aerosol properties over the oceans using POLDER/ADEAOS measurements. *IEEE Transact. Geoscience and Remote Sensing*, 37, 1586–1595.
- Herman, J. R., Bhartia, P. K., Torres, O., Hsu, C., Seftor, C., 1997a.** Global distribution of uv-absorbing aerosols from Nimbus 7/TOMS data. *J. Geoph. Res.*, 102, 16.911–16.922.
- Herman, M., Deuze, J.-L., Devaux, C., Golub, P., Bréon, F.-M., Tanré, D., 1997b.** Remote sensing of aerosols over land surfaces including polarization measurements and application to POLDER measurements. *J. Geoph. Res.*, 102, 17.039–17.049.
- Hess, M., Koepke, P., Schult, I., 1998.** Optical properties of aerosols and clouds : The software package OPAC. *Bull. Am. Met. Soc.*, 79, 831–844.
- Holben, B. N., Tanré, D., Smirnov, A., Eck, T. F., Slutsker, I., Abuhassan, N., Newcomb, W. W., Schafer, J. S., Chatenet, B., Lavenue, F., Kaufman, Y. J., de Castle, J. V., Setzer, A., Markham, B., Clark, D., Froin, R., Halthore, R., Karnieli, A., O’Neill, N. T., Pietras, C., Pinker, R. T., Voss, K., Zibordi, G., 2001.** An emerging ground-based aerosol climatology : Aerosol optical depth from AERONET. *J. Geoph. Res.*, 106, 12.067–12.097.
- Husar, R. B., Prospero, J. M., Stowe, L. L., 1997.** Charaterization of tropospheric aerosols over the oceans with the NOAA AVHRR optical thickness product. *J. Geoph. Res.*, 102, 16.889–16.909.
- IGOS, 2004.** For the monitoring of our environment from space and from earth. Technical report. GAW Report No. 159 (WMO TD No. 1235), ESA SP-1282, (IGOS : Integrated Global Observing Strategy). IPCC, 2002. Climate change 2001. the scientific basis. Technical report, Cambridge.
- Kasten, F., Young, A. T., 1989.** Revised optical airmass tables and approximation formula. *Applied Optics*, 28, 4735–4738.
- Kaufman, Y. J., Tanré, D., Gordon, H. R., Nakajima, T., Lenoble, J., Frouin, R., Grassl, H., Herman, B. M., King, M. D., Teillet, P. M., 1997a.** Passive remote sensing of tropospheric aerosol and atmospheric correction for the aerosol effect. *J. Geoph. Res.*, 102.
- Kaufman, Y. J., Tanré, D., Remer, L. A., Vermote, E. F., Chu, A., Holben, B. N., 1997b.** Operational remote sensing of tropospheric aerosol over land from Eos moderate resolution imaging spectrometer. *J. Geoph. Res.*, 102.
- Kaufman, Y. J., B. N. Holben, D. Tanré, I. Slutsker, A. Smirnov, and T. F.Eck (2000),** Will aerosol measurements from Terra and Aqua polar orbit-ing satellites represent the daily aerosol abundance and properties?, *Geo-phys. Res. Lett.*, 27, 3861–3864

- Kokhanovsky, A. A., Mayer, B., Rozanov, V. V., 2004a.** The account for the lambertian underlying surface reflection in problems of aerosol remote sensing. Atmospheric Research. Submitted.
- Kokhanovsky, A. A., von Hoyningen-Huene, W., Bovensmann, H., Burrows, J. P., 2004b.** The determination of the atmospheric optical thickness over western Europe using SeaWiFS imagery. IEEE Transac. Geosci. Remote Sensing, 42. In press.
- Kokhanovsky, A.A., 2004c.** Reflection of light from nonabsorbing semi-infinite cloudy media. A simple approximation. *J. Quant. Spectr. And Rad. Transfer* **85**, 25 – 33.
- Lee, K. H., Kim, J. E., Kim, Y. J., Kim, J., von Hoyningen-Huene, W., 2005.** Impact of smoke aerosol from Russian forest fires on atmospheric environment over Korea during may 2003. *Atmospheric Environment*, 39, 85–99.
- Lee, K. H., Kim, Y. J., von Hoyningen-Huene, W., 2004.** Estimation of regional aerosol optical thickness from satellite observations during the 2001 ACE-asia IOP. *J. Geoph. Res.*, 109.
- Moulin, C., Guillard, F., Dulac, F., Lambert, C. E., 1997.** Long-term daily monitoring of Saharan dust load over ocean using METEOSAT ISCCP-B2 data. *J. Geoph. Res.*, 102, 16.947–16.958.
- Nakajima, T., Higurashi, A., 1997.** AVHRR remote sensing of aerosol optical properties in the Persian gulf region, summer 1991. *J. Geoph. Res.*, 102, 16.935–16.946.
- Nakajima, T., Tanaka, M., 1988.** Algorithms for radiative intensity calculations in moderately thick atmospheres using a truncation approximation. *J. Quant. Spectrosc. Radiat. Transfer*, 40, 51–69.
- Olbert, C., 1998.** Atmospheric correction for CASI data using an atmospheric radiative transfer model. *Can. J. Remote Sensing*, 24, 114–127.
- Pollack, J. B., Cuzzi, J. N., 1980.** Scattering by nonspherical particles of size comparable to the wavelength : A semiempirical theory and its application to tropospheric aerosol. *J. Atmos. Sci.*, 37, 868–881.
- Rahman H. and Dedieu G. :** SMAC: a simplified method for the atmospheric correction of satellite measurements in the solar spectrum, *International Journal of Remote Sensing*, 1994, vol.15, No.1, 123-143.
- Rozanov, V. V., Buchwitz, M., Burrows, J. P., 2001.** SCIATRAN - a new radiative transfer model for geophysical applications in the 240-2400 nm spectral region : The pseudo-spherical version. *Advances in Space Research*. Submitted Oct. 2000.
- Rozanov, V. V., Diebel, D., Spurr, R. J. D., Burrows, J. P., 1997.** GOMETRAN: A radiative transfer model for the satellite project GOME, the plane-parallel version. *J. Geoph. Res.*, 102, 16.683–16.695.
- Santer, R., 2000.** Algorithm theoretical basis document: Atmospheric correction over land, MERIS ATBD 2.15. Technical report.
- Santer, R., Carrere, V., Dessailly, D., Dubuisson, P., Roger, J.-C., 2000.** MERIS ATBD 2.15 : Algorithm theoretical basis document, atmospheric correction over land. Technical report PO-TN-MEL-GS-0005, LISE.

- Santer, R., Carrere, V., Dubuisson, P., Roger, J.-C., 1999.** Atmospheric correction over land for MERIS. *Int. J. Remote Sensing*, 20, 1819–1840.
- Tanré, D., Remer, L. A., Kaufman, Y. J., Mattoo, S., Hobbs, P. V., Livingston, J. M., Russell, P. B., Smirnov, A., 1999.** Retrieval of aerosol optical thickness and size distribution over ocean from the MODIS airborne simulator during TARFOX. *J. Geoph. Res.*, 104, 2261–2278.
- Torres, O., P. K. Bhartia, J.R. Herman, Z. Ahmad, and J. Gleason, 1998:** Derivation of aerosol properties from satellite measurements of backscattered ultraviolet radiation: Theoretical basis. *J. Geophys. Res.*, 103, 17099–17110.
- Torres, O., Bhartia, P. K., Herman, J. R., Sinyuk, A., Ginoux, P., Holben, B., 2002.** A long-term record of aerosol optical depth from TOMS observations and comparisons to AERONET measurements. *J. Atmos. Sci.*, 59, 398–413.
- van der Meer, F., de Jong, S. M., 2000.** Improving the results of spectral unmixing of Landsat Thematic Mapper imagery by changing orthogonality of the end-members. *Int. J. Remote Sensing*, 21, 2781–2797.
- Vermote, E., F., Tanré D., Deuzé J.L., Herman M., Morcrette J.J., 1997,** Second Simulation of the Satellite Signal in the Solar Spectrum: an overview, *IEEE Transactions on Geoscience and Remote Sensing*, 35,3,675-686.
- Veefkind, J. P., de Leeuw, G., Durkee, P. A., Russell, P. B., Hobbs, P. V., Livingston, J. M., 1999.** Aerosol optical depth retrieval using ATSR-2 and AVHRR data during TARFOX. *J. Geoph. Res.*, 104, 2253–2260.
- von Hoyningen-Huene, W., Freitag, M., Burrows, J. P., 2003.** Retrieval of aerosol optical thickness over land surfaces from top-of-atmosphere radiance. *J. Geoph. Res.*, 108(D9), 4260–4279.
- von Hoyningen-Huene, W., Kokhanovsky, A. A., Freitag, M., Burrows, J. P., 2004.** Aerosol retrieval over land surfaces from multispectral nadir looking satellite measurements. In *SPIE* 5235. pages 366–374.
- von Hoyningen-Huene, Alexander A. Kokhanovsky, John P. Burrows, Prof. Dr.; Veronique Bruniquel-Pinel; Peter Regner, 2005a.** Simultaneous determination of aerosol- and surface characteristics from top-of-atmosphere reflectance using MERIS on board of ENVISAT. *J. Adv. Space Res.* 32(2005) (accepted).
- von Hoyningen-Huene, W., Kokhanovsky, A. A., Wuttke, M. W., Buchwitz, M., Gerilowski, N., Burrows, J. P., Latter, B., Siddans, B., Kerridge, B. J., 2005b.** Validation of SCIAMACHY top-of-atmosphere reflectance for aerosol remote sensing using MERIS L1 data. *ACP (Special Issue SCIAMACHY validation)*. Accepted 2004.
- von Hoyningen-Huene, W., 2005c:** Cloud influence on satellite measurements of aerosol properties. In ACCENT AT-2, Report of the 3. AT-2 Workshop, Oberpfaffenhofen, 6.-8 June 2005, p. 45-50. [http://troposat.iup.uni-heidelberg.de/AT2/workshop/AT2\\_wks\\_3\\_report.pdf](http://troposat.iup.uni-heidelberg.de/AT2/workshop/AT2_wks_3_report.pdf)
- Zimmermann, G., 1998.** MOS ground truth program - instruments - campaigns - results. In *2<sup>nd</sup> International Workshop on MOS-IRS and Ocean Colour*. Number ISBN 3-89685-559-X, DLR, Berlin, pages 13–38.